Biomineralization-Inspired Material Design for Bone Regeneration

ADVANCED HEALTHCARE MATERIALS
www.advhealthmat.de

Biomineralization-Inspired Material Design for Bone Regeneration

*Daniel de Melo Pereira and Pamela Habibovic**

Synthetic substitutes of bone grafts, such as calcium phosphate–based ceramics, have shown some good clinical successes in the regeneration of large bone defects and are currently extensively used. In the past decade, the field of biomineralization has delivered important new fundamental knowledge and techniques to better understand this fascinating phenomenon. This knowledge is also applied in the field of biomaterials, with the aim of bringing the composition and structure, and hence the performance, of synthetic bone graft substitutes even closer to those of the extracellular matrix of bone. The purpose of this progress report is to critically review advances in mimicking the extracellular matrix of bone as a strategy for development of new materials for bone regeneration. Lab-made biomimicking or bioinspired materials are discussed against the background of the natural extracellular matrix, starting from basic organic and inorganic components, and progressing into the building block of bone, the mineralized collagen fibril, and finally larger, 2D and 3D constructs. Moreover, bioactivity studies on state-of-the-art biomimicking materials are discussed. By addressing these different topics, an overview is given of how far the field has advanced toward a true bone-mimicking material, and some suggestions are offered for bridging current knowledge and technical gaps.

1. Introduction

1.1. Bone Graft Substitutes

Currently, over 2 million bone grafting procedures are performed annually worldwide, and this number is predicted to increase.[1]

Autologous bone grafting is the current standard of care for bone defects that do not heal spontaneously for a variety of reasons. The structural organization of a patient's own tissue provides an environment for osteoconduction (migration of osteogenic host cells into the transplanted material), its chemical composition and associated growth factors support osteoinduction (induction of differentiation of undifferentiated stem cells into osteoprogenitor cells), and it contains progenitor cells that are able to initiate osteogenesis (forming bone from the interior of transplanted material). In addition to that, autologous bone poses virtually no risk of immunogenic response.[2]

The drawbacks of the use of autologous bone grafts are tied with the finite supply (5–70 cm^3) as well as with the harvesting procedure. The graft is usually taken from the iliac crest, a procedure that is associated with minor (10–39% of cases) and major (0.76–25% of cases) complications. A relatively new method using a reamer–irrigator–aspirator (RIA) device harvests bone fragments from the intramedullary canal with potentially lower complication rates (overall 6%); however, this method is not yet as widespread as harvesting from iliac crest bone.[3]

Eliminating the autologous harvesting procedure by using bone graft substitutes is obviously very attractive, and alternatives including allogeneic grafts (human derived), xenogeneic grafts (animal derived), or synthetic bone graft substitutes are abundantly described in the literature, and are also used in the clinical setting.[4,5] Allogeneic and xenogeneic bone grafts suffer from disadvantages related to their origin, being the risk of immune reactions and disease transmission. Synthetic bone graft substitutes lack these drawbacks and have the potential to perform as well as autologous bone graft, but have the additional challenge of doing so while remaining affordable.

The affordability issue precludes, to some extent, the use of cell- and growth factor-based tissue engineering scaffolds despite some clinical successes.[6–9] Other associated drawbacks are related to cell survival upon implantation,[10] and diffusion of growth factors into surrounding tissue, possibly causing ectopic bone formation that may lead to complications and often requires surgical intervention.[11–13]

A systematic review on biomaterial-based bone graft substitutes for use in the orthopedics, performed in the UK showed that only 4 out of 59 commercially available products were demonstrated to perform equally or better than bone autograft.[4] These products were Alpha-BSM (DePuy),[14,15] a resorbable calcium phosphate paste, Cortoss (Orthovia),[16] a nonresorbable bioactive glass cement, Vitoss (Orthovia),[17] a resorbable composite of calcium phosphate and collagen, and Norian SRS (Synthes),[18] a resorbable CaP cement. Strikingly, Vitoss is the only product showing signs of osteoinduction, a property

D. de Melo Pereira, Prof. P. Habibovic
MERLN Institute for Technology-Inspired Regenerative Medicine
Maastricht University
P.O. Box 616, 6200 MD Maastricht, The Netherlands
E-mail: p.habibovic@maastrichtuniversity.nl
The ORCID identification number(s) for the author(s) of this article can be found under https://doi.org/10.1002/adhm.201800700.

DOI: 10.1002/adhm.201800700

considered essential for successful bone regeneration of large bone defects. Also important to note is that most of the products available are based on calcium phosphates, the exception being the bioglass cement, which has similar properties to CaPs in that it possesses tunable degradability and allows direct contact with bone tissue. Despite the proven bioactivity, none of these materials are able to sustain loads by themselves, and therefore they are typically used in combination with (metallic) fixation instruments.[4]

This is the current challenge for bone graft substitutes: having load-bearing capacity comparable to cortical bone, sufficient bioactivity (osteoconduction and induction) to elicit new bone formation, and degrading as it is replaced by newly formed native tissue.[19] All these properties are combined in the natural bone tissue, originating from its composition and hierarchical structural organization. Natural bone is therefore a logical source of inspiration for developing novel biomaterials for bone repair and regeneration.

1.2. Aim

What is the state of the art in developing nature-inspired/biomimetic bone graft substitutes and what are the promises for the future?

These are the main questions that this review aims to answer, by critically analyzing recent developments in the biomaterials field, inspired from advances in the field of biomineralization, leading to materials that are close to natural bone in structure and composition. The goal is to comprehensively cover the strategies to reproduce various properties of extracellular bone matrix, ranging from the chemical composition of the mineral phase to mechanical properties stemming from 3D hierarchical structures. The key challenges that need to be tackled at each length scale are highlighted as well as possible ways to overcome them.

To provide adequate background, the next section contains a short introduction to the extracellular matrix (ECM) of bone as context for discussion of achievements in bone-mimicking biomaterials research and development.

1.3. Bone Structure and Composition

Regarding the composition and structure of bone, it is important to recall that the focus is on secondary, or lamellar bone, in contrast to primary or woven bone. Secondary bone is found in mature bones, in the form of cortical (dense, compact) or cancellous (spongy, trabecular) bone. The lamellar bone tissue is remodeled from primary bone, which can be formed by endochondral ossification (mineralization of preexisting cartilage template) or by intramembranous ossification (direct bone formation).

The overall composition of the extracellular matrix of bone, excluding the various cell types that populate the matrix, is about 25 wt% organic component, 65 wt% inorganic component, and 10 wt% water content. Water is found in pores and channels within the bony matrix (5–20% of the total water present in bone), as well as in close association with the collagen fibrils and apatite mineral. In particular the latter, bound water, contributes to the plastic behavior of bone and its ability to absorb energy, with a decrease in water content due to aging resulting in a lower resistance to fracture.[20] Starting from basic components to a whole bone, an overview of structure and organization of the matrix is given below.

Daniel de Melo Pereira is a Ph.D. candidate at the Instructive Biomaterials Engineering Department at Maastricht University's MERLN Institute in The Netherlands. He studied biomedical engineering at the University of Coimbra, Portugal, and his research interests include biomimmetic materials, biomineralization, and design of materials for bone regeneration.

Pamela Habibovic is currently a Professor of Inorganic Biomaterials and chair of the Instructive Biomaterials Engineering Department at MERLN Institute, Maastricht University, The Netherlands. Her research group focuses on synthetic biomaterials for regenerative medicine. Different research lines include (ceramic) bone graft substitutes, biomimmetic materials, bioinorganics, nanomaterials for targeted delivery, and microfluidic-based (high-throughput) screening approaches for biomaterials research.

1.3.1. Organic Phase

The organic matrix of bone comprises around 90 wt% type I fibrillar collagen and 10 wt% noncollagenous proteins. Collagen molecules aggregate in triple helices—tropocollagen—that are 300 nm long and 1.5 nm wide. These are stacked longitudinally with a gap of 40 nm, and having a lateral spacing of 1–2 nm.[21] A collagen fibril (about 100 nm in diameter) is made up of staggered rows of axially packed, tropocollagen molecules with lateral crosslinks (**Figure 1**).[22] These crosslinks can be enzymatic or nonenzymatic. The enzymatic links are further divided into immature (divalent) and mature (trivalent) crosslinks, and their total amount and ratio are related to the mechanical properties of bone, such as stiffness, tensile strength, and fracture toughness. The nonenzymatic crosslinks result from accumulation of advanced glycation end (AGE) products and are correlated with increased bone brittleness in aging or disease.[23] The staggering of rows creates periodic density variations in the

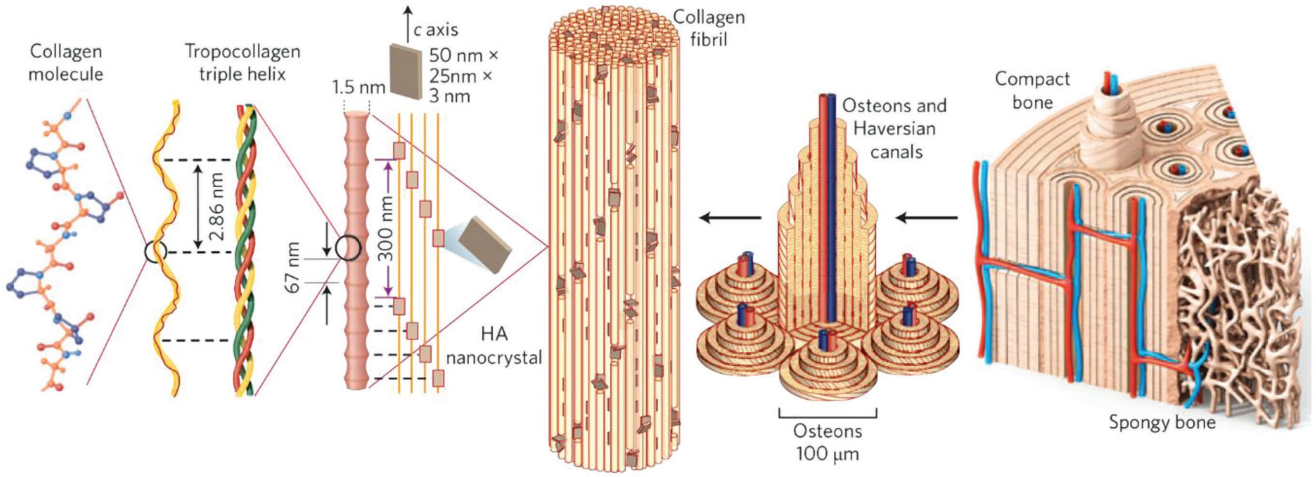

Figure 1. Schematic of the hierarchical structure of bone. Collagen molecules, with unique amino acid sequence, are assembled into triple helices, forming what is known as a tropocollagen molecule. Tropocollagen molecules come together with apatite crystallites in the collagen fibril, the building block of bone. Collagen fibrils further associates into bundles, lamellae, and finally osteons, the microscale structure of bone. Trabecular or spongy bone is porous and resides in the interior of, for example, long bones, while the compact bone is much less porous and is present at the exterior. Reproduced with permission.[148] Copyright 2015, Nature Publishing Group.

fibril, visible in transmission electron microscopy (TEM) due to the misalignment of the gaps between molecules.[24] These nanoscale spaces within the collagen fibril are templates that are populated by mineral during bone formation.

While collagen is the main organic component of the extracellular matrix, the matrix contains a multitude of other noncollagenous proteins (NCPs). The roles of these proteins are still not completely understood; for a comprehensive overview of the available knowledge of these proteins we refer to the review by Zhu et al.[25] **Table 1** highlights the NCPs that are thought to have a structural role (i.e., they are present in the matrix at some point) in the formation and regulation of the extracellular matrix. This excludes enzymes (e.g., alkaline phosphatase despite its role in phosphate liberation) or growth factors (e.g., bone morphogenetic proteins despite their role in promoting mineralization). Most NCPs have a regulatory function in the process of biomineralization, but some also have direct implications for the mechanical properties of bone. Osteopontin (OPN) is hypothesized to play a role in preventing crack propagation: OPN-deficient mice showed 30% less resistance to fracture.[26] OPN and osteocalcin were furthermore shown to influence the formation of sub-micrometer gaps, called dilational bands, between adjacent mineral aggregates. The formation of these dilational bands was correlated with diffuse damage at the micrometer scale and increased resistance to fracture.[27]

1.3.2. Mineral Phase

Bone mineral, or bone apatite, can be found inside the collagen fibril (intrafibrillar mineral) as well as surrounding it (extrafibrillar mineral) although their relative fractions are a matter of dispute.[28,29] In a recently published analysis of the morphology of the mineral particles, obtained by 3D reconstruction of tomography data from ion-milled bone slices, imaged by scanning transmission electron microscopy, classification in four hierarchical categories was made. Thin (5 nm base), elongated (50–100 nm) and curved crystals aggregate laterally (width 20–30 nm) to form the platelets often described in literature.[30] These can be further organized into thicker stacks of two to four platelets, or into aggregates of all the previous structures, forming complex shapes up to 300 nm.[31]

The chemical composition of bone apatite is far from the stoichiometric hydroxyapatite as it is highly substituted with ions from the physiological fluids. These substitutions can occur in any of its four crystallographic domains: the PO_4^{3-} tetrahedral positions, the Ca^{2+}(I) positions (phosphate surrounded hexagonal columns) or Ca^{2+}(II) positions (staggered triangular surrounding hydroxide) or in the OH^- "channel" positions.[32] The precise composition of ion substitutes tends to vary among subjects and depending on the type of bone itself, but in general the following ions are present: CO_3^{2-} (around 5 wt%), Na^+ and Mg^{2+} (both between 0.5 and 1 wt%),[30,33,34] K^+, Sr^{2+}, Cl^-, F^- (up to 0.1%), and trace amounts (in the ppm range) of several other metallic elements: B, Al, Si, Ti, Cr, Mn, Fe, Co, Zn, Sr, Cd, La, and Pb.[35–37] There is debate about whether the crystallographic unit cell is hexagonal or monoclinic.[30,38]

Mineral platelets are hypothesized to be closely related to the citrate anion, which is present in high concentration in bone.[39] The role of citrate is not yet well defined although evidence exists relating it to the restriction of apatite crystal growth[40,41] and to the stabilization of an amorphous calcium phosphate phase.[42]

1.3.3. Mineralized Collagen Fibril

The components described so far, the structural collagen matrix, noncollagenous proteins and molecules, and the apatite platelets, come together in what is considered to be the building block of the extracellular matrix of bone: the mineralized collagen fibril (Figure 1).[148]

Table 1. Noncollagenous structural proteins involved in the formation or regulation of the extracellular matrix.

Noncollagenous protein	Known or hypothesized role
Large proteoglycans	
Versican (VCAN)	Present in early stages of bone development.[149] Contains EGF-like sequences that may affect osteogenic differentiation.[150,151]
Small leucine-rich repeat proteoglycans (SLRPs)	
Decorin (DCN) and biglycan (BGN)	Regulators of collagen fibrillogenesis.[152,153] Decorin possibly modulates collagen mineralization.[154] Biglycan is involved in angiogenesis during fracture healing,[155,156] and osteoblast differentiation.[157]
Osteomodulin (OMD)	Involved in the organization of the collagen matrix.[158]
Asporin (ASPN)	Possible role in collagen mineralization.[159,160]
Fibromodulin (FMOD) and lumican (LUM)	Involved in the organization of the collagen matrix.[161]
Glycoproteins	
Osteonectin (SPARC)	Affinity to collagen and hydroxyapatite, involved in collagen mineralization.[162,163]
Tetranectin (CLEC3B)	Possibly involved in fracture healing.[164]
RGD-containing glycoproteins	
Thrombospondin-2 (THBS2)	Involved in the organization of the collagen matrix.[165]
Fibronectin (FN1)	
and vitronectin (VTN)	Possibly providing attachment points to various cell types.[166]
Small integrin-binding ligands with N-linked glycosilation (SIBLINGs)	
Osteopontin (SPP1)	Affinity to collagen and hydroxyapatite, known inhibitor of ectopic calcification, modulator of bone mineralization.[167]
Bone sialoprotein (IBSP)	Affinity to collagen and hydroxyapatite, induces differentiation of osteoblasts and is a mineralization promoter.[168,169]
Dentin matrix protein 1 (DMP1)	Involved in bone mineralization, likely promoter of mineralization.[51,170]
Matrix extracellular phosphoglycoprotein (MEPE)	Involved in bone mineralization, likely inhibitor of mineralization.[171–173]
Bone acidic glycoprotein 75 (BAG-75)	Possibly involved in early stages of bone mineralization.[174–176]
γ-Carboxy glutamic acid proteins	
Matrix gla protein (MGP)	Inhibitor of mineralization.[177,178]
Osteocalcin (BGLAP)	Regulator of mineralization.[173,179,180]
Serum proteins	
Albumin (ALB) and α_2-HS-glycoprotein (AHSG)	Both have affinity to Ca^{2+}, inhibiting hydroxyapatite mineralization by arresting crystal growth. AHSG does so to a greater extent than albumin.[181,182]

The small dimensions of crystallites, their highly substituted chemical phase, and close associations with collagen and other organic molecules make it rather difficult to precisely characterize this unit block although more is known about its composition (described in the previous section) than about the mechanisms by which it is formed. The 3D arrangement of apatite and collagen at the nanoscale has also been recently described.[31]

The mounting evidence for amorphous precursors in the formation stages of bone from different vertebrates, namely in zebrafish fin rays,[43–45] mouse calvaria and long bones,[46,47] as well as in enamel in mouse,[48] points toward a nonclassical mineralization pathway.[49] This is substantiated with an in vitro study on the formation of amorphous calcium phosphate (ACP) that correlates with the ACP phase found in vivo.[50] The process of collagen mineralization by an amorphous precursor is likely assisted by NCPs that stabilize ACP and interact with collagen, as shown in in vitro models for DPP, DMP1,[51,52] OPN,[53] and AHSG,[54–56] as well as by a study on remineralization of DBM.[57] Carbonate has also been hypothesized to have a role in the formation of first mineral domains, but at the moment only limited in vitro evidence exists.[58–60] Therefore, much is still to be discovered about the mechanisms of mineralization regulated by organic components.[61]

1.3.4. Fibril Arrays, Lamella, and Osteons

Mineralized collagen fibrils (about 100 nm) bundle together in fibril arrays (sometimes called fibers), and these are arranged in parallel stacks. A lamella consists of typically parallel fibril arrays (in the range of 100 nm to 10 µm). Lamella can be stacked in different ways,[62] for example, in parallel stacks, with a slight angle offset, or alternating at sharp angles.[63,64]

Osteons are the hallmark structure of secondary bone, and they have a diameter of around 100 µm. An osteon consists of a central (Haversian) canal, occupied by a blood vessel, and surrounded by concentric lamella (Figure 1). Canals perpendicular to the Haversian canal, the so-called Volkmann canals, link adjacent osteons. Lacunae, with resident osteocytes, populate the bone surrounding the Haversian canal, with their long axis concentric to the Haversian canal. Canaliculi extend from the lacunae, linking adjacent osteocytes to each other and to a filtering surface.

1.3.5. Cortical and Trabecular Bone

Cortical bone forms the hard shell–like surface of a bone, while trabecular bone fills its core. Porosity distinguishes cortical (≈6%) and trabecular bone (≈80%)). While osteons are packed together in cortical bone, in trabecular bone the mineralized matrix is sparse, consisting of interconnected struts of about 200 µm (Figure 1). These trabeculae undergo constant remodeling, and their orientation and local density depend on the typical load applied to the bone.[21] The pores in this sponge-like structure house the bone marrow.

2. Biomineralization-Inspired Materials

In the following section, examples of biomaterials are given that possess closer-to-bone characteristics. The focus is on discussing the state-of-the-art of bone-mimicking or bone-inspired biomaterials, and having a critical comparison of such materials with the natural extracellular matrix.

2.1. Mimicking the Building Block of Bone

When ascertaining to what level an artificially produced mineralized collagen fibril replicates the building block found in natural bone, there are several key points to keep in mind (**Figure 2**). One is the high mineral content of the natural nanocomposite, of around 65 wt%, that can, for example, be shown by thermal gravimetric analysis (TGA) (Figure 2g). The second is a homogenous mineralization throughout the developed substrate that can be demonstrated using elemental surface analysis methods such as energy-dispersive X-ray spectroscopy (EDS) mapping performed on different areas (Figure 2b–c). Third, there must be evidence of the close relationship between the apatite mineral and the collagen matrix, which can be observed by scanning electron microscopy (SEM) and EDS, or TEM. Fourth, proof that mineralization is intrafibrillar, which can be obtained by a combination of indirect methods, or directly, by the use of 3D imaging techniques. Indirectly, intrafibrillar mineralization can be evidenced by a combination of techniques that show that the composite has a high mineral content (e.g., TGA), while the normal ultrastructure and surface of the organic matrix is maintained (e.g., SEM-EDS), leading to the conclusion that the mineral must reside within the organic matrix. The latter analysis should show that at early time points, no extrafibrillar mineral is present, as mineralization typically starts from the inside out, leaving the collagen surface unaltered (Figure 2a). Unequivocal proof of intrafibrillar mineralization can be obtained with 3D imaging techniques such as cryogenic electron tomography (Figure 2h) or, alternatively, by clever use of super-resolution microscopy techniques such as stochastic optical reconstruction microscopy, used to image fluorescent calcein-labeled apatite, to show its localization within immuno-labeled collagen fibrils (Figure 2i). Last, it is important to show that the mineral present is similar to bone apatite, in composition, particle size and orientation. Data from selected-area electron diffraction (SAED) in combination with TEM imaging covers all three, by revealing the angles and d-spacing characteristic of apatite mineral and proving that the orientation of the crystallographic *c*-axis is along the longitudinal axis of the collagen fibril (Figure 2d–f).

In the context of reconstituting the main building block of bone, i.e., the mineralized collagen fiber, the discovery of the so-called polymer-induced liquid precursor (PILP) process has had a major impact. This process, which was observed in the in vitro experiments on the stabilization of amorphous mineral phases, was initially described for calcium carbonate[65] and later for CaP.[30] The PILP process encompasses, in the case of CaP, the stabilization of hydrated clusters of $Ca_2(HPO_4)_3^{2-}$ that form from saturated solutions,[50] by charged (typically anionic) polymers, effectively creating stable amorphous calcium phosphate–polymer particles.

The ACP–polymer complexes are capable of infiltrating preassembled collagen fibrils through the a-band of the 40 nm gap region of collagen.[56] The mineral then crystallizes inside the fibril, resulting in mineralized collagen fibrils that have a remarkable resemblance to mineralized collagen found in natural bone. More specifically, the intrafibrillar mineral consists of crystallites with the *c*-axis orientation in the direction of the fibril.[30] The exact mechanism of infiltration is still under debate, and various hypotheses suggest the importance of electrostatic interactions,[50,56] capillary-like forces,[30] mineralization by inhibitor exclusion,[55] or simultaneous fibrillogenesis and apatite formation.[66] Interestingly, the fact that intrafibrillar mineralization of collagen was achieved via an amorphous precursor in vitro prompted the biomineralization community to renew efforts in investigating the role of such precursors in the in vivo biomineralization process. These efforts resulted in the confirmation that indeed, in the process of formation of zebrafish fin rays, and mouse calvaria, long bones, and enamel, an amorphous precursor is present, as mentioned in the introductory section.[43,45–48,67] Since early 2000, a range of experiments have been performed that have increased our understanding of the process of intrafibrillar mineralization of collagen and bone biomineralization, as well as provided useful tools for developing truly biomimetic materials for bone regeneration.

A large majority of approaches to obtain intrafibrillar collagen mineralization employs polymeric process-directing agents; however, in a few studies the process was performed in the absence of NCPs or their analogs. For example in a study by Wang et al., the authors employed simultaneous collagen fibrillogenesis and precipitation of carbonated apatite. This approach proved capable of forming intrafibrillar mineral, with orientation of the crystallographic *c*-axis in the collagen fibril direction, as shown by TEM-SAED and SEM microscopic images. The mineral content, determined using TGA, was 32 wt% after a 4 day reaction (calculated relative to the dry composite, taken as wt% left at 200 °C). The mineralization was extended by a 16 day immersion in a simulated body fluid, resulting in an increase of mineral content up to 50 wt% of the dry mass.[66] While this work proved that NCPs, or their analogs are not necessary to achieve intrafibrillar mineralization of collagen, the mineralization extent in this study falls somewhat short of the expected 65 wt%. Furthermore, while it is expected that the mineral deposited during the first phase is homogeneously spread throughout the scaffold, this is less certain for

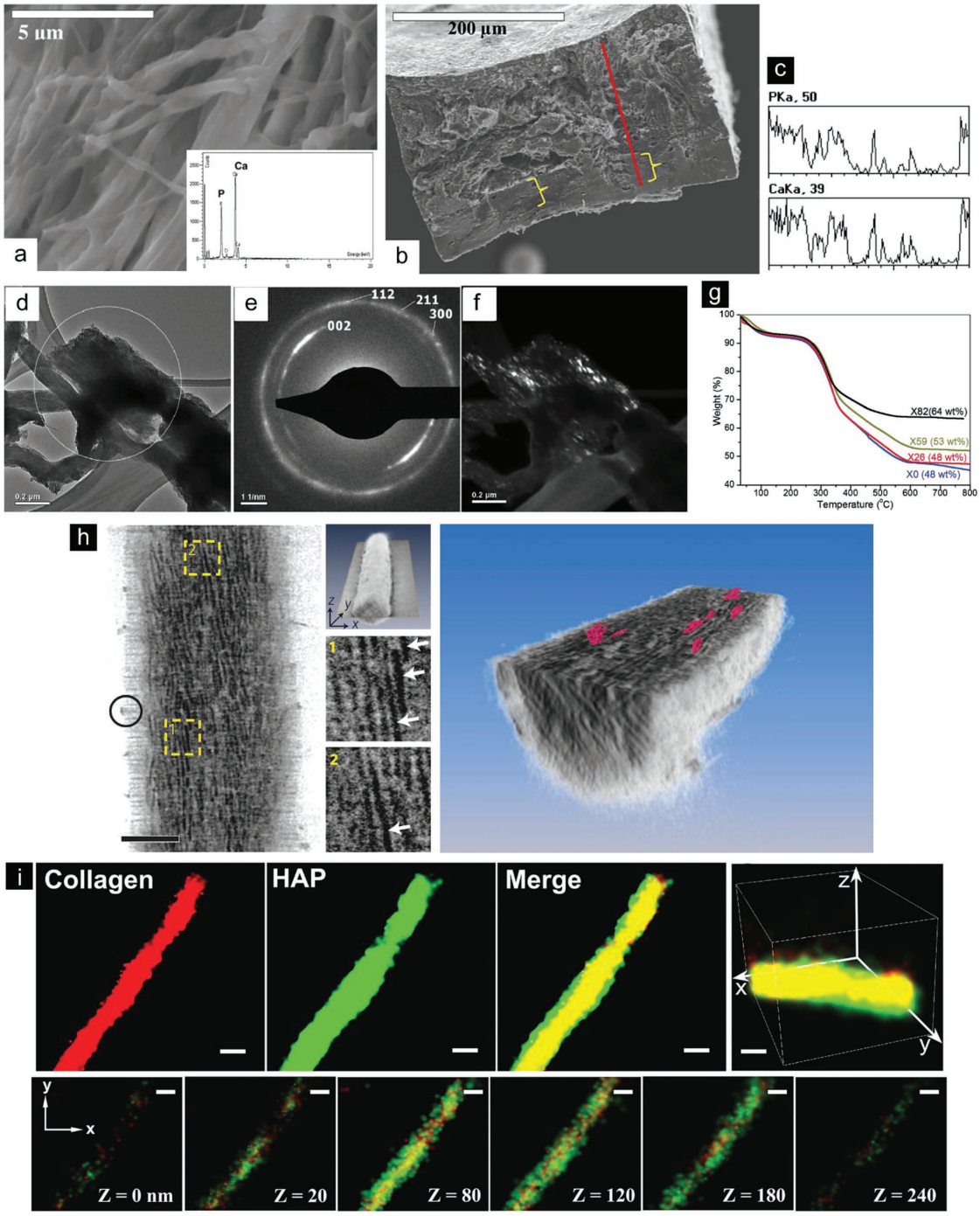

Figure 2. Characterization of intrafibrillar-mineralized collagen. a) SEM image of a collagen scaffold mineralized for 3 days, showing a typical surface morphology of the organic matrix, while EDS spectrum (inset) shows the presence of Ca and P, associated with CaP mineralization; b) SEM image of a remineralized piece of manatee bone, with c) EDS spectra collected along the red line, showing heterogeneous Ca and P distribution on the cross section, suggesting that infiltration of the pAsp–ACP complex was not complete; d) bright field TEM image of a mineralized collagen fibril and e) corresponding SAED pattern, showing characteristic 002 reflection aligned with the fibril, and ring composed of the 112, 211, and 300 reflections; f) dark field TEM image made with the beam from the 002 reflection, showing crystals distribution within the collagen fibril; g) TGA of PILP-mineralized collagen sponges showing that increasing degree of crosslinking (X0: control; X26 < X59 < X82) promotes increase in mineral content; h) cryo-ET of a mineralized collagen fibril showing the plane of section through the middle of the fibril, with magnified regions identified by yellow squares, where apatite platelets are visible as dark streaks (white arrows). On the right a 3D reconstruction of the apatite platelets embedded in the collagen fibril: i) STORM images of calcein-labeled apatite (red) and immunostained collagen (green), imaged in a *z*-stack ranging 0–240 nm, showing the presence of apatite within the collagen fibril. (a) Reproduced with permission.[77] Copyright 2010, Elsevier. (b,c) Reproduced with permission.[69] Copyright 2011, Elsevier. (d–g) Reproduced with permission.[80] Copyright 2011, American Chemical Society. (h) Reproduced with permission.[56] 2010, Nature Publishing Group. (i) Reproduced with permission.[97] 2018, Wiley-VCH.

the second phase, where the substrate is already dense and mineralized before immersion in the SBF solution. Indeed, cryo-TEM microscopic images of the scaffold showed fibrils ranging from not mineralized to fully mineralized. Complementary SEM-EDS analyses at different depths across the 3 mm thick disc would have given a valuable insight in the homogeneity of mineral distribution throughout the dense substrate.

In another study by Marelli et al., it was hypothesized that the pH at which collagen fibrils are formed influences intrafibrillar mineralization. Using cationic or anionic dyes, it was confirmed that collagen gels formed under mild alkaline conditions (pH = 9.0) had more negative charges than gels formed under neutral conditions (pH = 7.4). After mineralization in SBF for 14 days, the negatively charged gel had 64 wt% more mineral deposited than the positively charged one. Although this was presented as intrafibrillar mineral, no conclusive evidence was provided to support this statement. The TEM image of the gel after 24 h of incubation in SBF showed mineral agglomerates together with a collagen fibril, but the exact location of the mineral (adjacent to, on top of, or inside the fibril) was not clear. The supplementary SEM images strongly suggested that the mineral formed was actually extrafibrillar, and the authors were careful to phrase the figure captions as "mineral formation within the collagen framework," which suggests that the formation occurred inside the collagen gel, but that it was not necessarily intrafibrillar.

Among the different polymeric additives that have been explored in the context of mineralization with process-directing agents, poly(aspartic acid) (pAsp) is the most commonly used.[30,52,56,57,68–80] Other polymer additives include poly(glutamic acid) (pGlu),[79,81,82] poly(amidoamine) dendrimers,[83,84] poly(acrylic acid) (PAA),[69,81] typically used in combination with poly(vinylphosphonic acid) (PVPA),[79,81,85,86] sodium trimethaphosphate (STMP),[87] poly(glutamic acid),[88] or phosphorylated collagen.[89,90] The only example of a cationic polymer able to induce intrafibrillar mineralization of collagen is the one of poly(allylamine) hydrochloride (PAH).[61,91–93]

It is hypothesized that the high content of anionic side chains in, e.g., pAsp, as well as its nonglobular, flexible nature, mimics the composition and structure of certain acidic NCPs found in vivo such as OPN, DMP1 and DPP, known to be involved in biomineralization processes.[94,95] These are classified as intrinsically disordered proteins that have a high content of charged side chains and lack a well-defined tertiary structure. However, not all aspects of the NCPs are present in polymeric analogs: often they lack the integrin- or collagen-binding sequences, phosphorylated serine/threonine content, or post-translation modifications such as glycosylation, and the role of these NCP motifs in biomineralization remains elusive.[96] The exception is perhaps the role of phosphorylated side chains, which were mimicked by the use of PVPA as process-directing agent, or by pretreating collagen with STMP. PVPA, either in solution or crosslinked to collagen, was able to induce intrafibrillar mineralization of reconstituted collagen fibrils and demineralized dentin, but only in the presence of PAA.[81,86] The phosphorylation of collagen fibrils by SMTP before immersion in a mineralization solution (stabilized by PAA) was also shown to produce intrafibrillar mineral in reconstituted fibrils and demineralized dentin.[85,87]

These studies seem to suggest that the use of phosphorylated groups has a role in guiding the formation of intrafibrillar mineral, but not in stabilizing ACP itself, as this was accomplished by another biomimetic analog (PAA). The lack of quantification of mineral content in the collagenous matrix, for example by TGA, makes comparison with other mineralization strategies difficult. Moreover, the rather complicated mineralization setup used in these studies, consisting of a combination of set Portland cement (as Ca^{2+} and OH^- source) and a modified SBF (as PO_4^{3-} source), as well as the necessary use of two biomimetic analogs makes this strategy rather complex for the results it yields.

Comparative studies on the effect of polymer concentration[79] and molecular weight[77] point toward pAsp of high molecular weight (highest reported is 32 kDa, but 27 kDa is more commonly used) as the best process-directing agent for achieving mineral content between 60 and 70 wt%, comparable to that of native bone. Similar ranges of mineral content were obtained by combinations of pGlu with pAsp, but there was no added benefit from the incorporation of pGlu.

The influence of polymer concentration is harder to gauge from the existing literature, because for many studies, the reaction volume is not stated, and similar mineral content (wt%) is achieved with different concentrations, ranging from 10 to 100 μg mL^{-1}. One study analyzed the effect of concentration of pAsp (molecular weight 2–11 kDa) below 10 μg mL^{-1}, finding that the rate of infiltration and mineralization slowed down with increasing concentration of the process-directing agent.[52] However, these results were obtained for collagen fibrils reconstituted on TEM grids, and the mineralization solution was less concentrated than typical PILP preparations (2.7×10^{-3} M $CaCl_2$ and 1.35×10^{-3} M K_2PO_4), making the comparison with other studies that often use bulk reactions for millimeter-sized substrates difficult.

Another aspect that has been shown to affect the mineral content upon PILP-driven mineralization is the extent of collagen crosslinking. For example, it has been demonstrated that a collagen sponge exhibited increased mineral content (48, 53, and 64 wt%) with an increase in crosslink density (26%, 59%, and 82% of free amine groups in collagen).[80] The mineralization reaction of a 10 mg reconstituted collagen sponge using 10.5 kDa pAsp (50 μg mL^{-1} in 100 mL) lasted for 14 days. When a (non-crosslinked) commercial sponge was used, the same level of mineralization was achieved after 16 days; however, in the latter case, the reaction volume used was 5 times higher (10.3 kDa pAsp (50 μg mL^{-1} in 500 mL)).[77] Taken together, these studies suggest that the crosslinking of collagen substrates is an efficient way of improving mineralization kinetics. Moreover, crosslinking density was correlated with increasing stiffness and hardness of the composite, with the highest crosslink density (82%) showing elastic modulus comparable to that of woven bone (around 0.2 GPa), even in the wet state.[80]

In a recent study by Shao et al., citrate was also shown to increase the mineral content of reconstituted collagen and demineralized dentin, when used in combination with pAsp-assisted mineralization. Collagen gels were pretreated in a citrate-containing solution, before immersing in mineralization medium, and showed increased residual mineral wt% with increasing concentration of citrate.[97]

One aspect that has not been extensively discussed or investigated is the influence of the nature or properties of the collagen substrate itself on the mineralization by the PILP process. It is known that the nanometer-sized compartments, created during fibrillogenesis, and discernible through the emergent 67 nm periodic *D*-spacing, are necessary for infiltration of the hydrated complexes, and also have a role in directing crystallization and determining the final morphology of the apatite mineral.[56] Proper fibril formation appears to be the only necessary condition for subsequent intrafibrillar mineralization. However, the collagen scaffolds used in the studies reported here have many different origins and have undergone different processing. For example, collagen substrates have been used as reconstituted fibrils or sponges (sometimes called membranes) from acid- or enzyme-extracted collagen (that can be prepared in-house or purchased). They can originate from rat-tail tendon,[61,75,91] bovine[77,79,90,92,93] or equine tendon,[52,56] or bovine skin.[30,68,80,81,83,85] Substrates have also been prepared directly from biological tissue, such as turkey tendon,[78] demineralized sections from mouse periodontium,[57] and bone from manatee,[69,79] or fish[82] origin, as well as demineralized dentin from mouse,[72,73] or human origin.[70,71,74,86–89]

The versatility of the PILP process is attested by the mineralization results with all these substrates. But considering the differences between the reactions employed—conditions of fibril formation, molecular weight and concentration of the additive, reaction volume and time—one may question whether there is an underlying relation between the conditions required for successful mineralization and the properties of the substrate. In other words, are we simply selecting the conditions that work for a certain substrate, but missing some key aspect in the overall mechanism? This is supported by sporadic observations of heterogeneity of mineral deposition, more so in reconstituted than in tissue-derived collagen; and also by (possibly underreported) failed mineralization reactions upon aging of a collagen substrate known to have worked previously.[96] With the available information, this conclusion remains speculative, and therefore, more systematic studies are needed on the influence of collagen origin and processing on the efficiency and kinetics of mineralization.

In addition to pAsp and other polymers described above, whole (recombinant or purified) proteins have also been used for collagen mineralization studies, as mentioned in Section 1.[51,53–56] Inspired by the native proteins, some tailor-made peptides and proteins have been developed and shown to play a role in CaP precipitation in vitro,[98] although a few attempts have been made to use them as NCP analogs in collagen mineralization studies. Sfeir et al. used a peptide containing a DPP-like motif, giving some insight into the possible phosphorylation mechanism of sequential serine residues, often found in NCPs.[99] Ping et al. used a multifunctional protein, containing a BSP-sequence and an HAP-binding motif that was shown to promote intrafibrillar mineralization of collagen in the presence of poly(acrylic acid).[100] These studies have made an important contribution to the existing knowledge regarding the mechanisms of bone mineralization. Nevertheless, the number of studies in which tailor-made NCP analogs like these have been used to develop in vitro building blocks of bone is much lower than the studies where the far simpler synthetic polymers described above were used. Furthermore, the extent of mineralization obtained using these methods seemed to be inferior to, e.g., pAsp-driven mineralization.

Taken together, it can be concluded that our knowledge of the roles and importance of NCPs is still relatively limited. Nevertheless, continued research on biomineralization-related synthetic peptides and proteins is warranted as such compounds may be useful in controlling, for example, the extrafibrillar mineral formation, in enhancing mechanical properties of synthetic bone substitutes, but also in less obvious ways, as replacements of collagen as the structural matrix, as described in Section 2.3.

2.2. Mimicking the Biological Apatite

Where the previous section focused on the methods to replicate the intimate contact between apatite and collagen, here we zoom in into the properties of the mineral phase formed during intrafibrillar mineralization of collagen. It should be noted that while a large body of literature exists on methods to produce bone-like apatite (e.g., described in several reviews[101,102]), here only the studies concerning mineral formed during intrafibrillar mineralization of collagen are discussed. In the previous section, it was shown that some excellent results were obtained on the nanoscale organization of organic and inorganic constituents of bone-like building blocks by using intrafibrillar mineralization of collagen. In contrast, less is known about the chemical composition of the deposited mineral phase, specifically regarding ionic substitutions. Characterization of intrafibrillar mineral is mostly limited to TEM-SAED and X-ray diffraction (XRD) data, showing crystallite size and orientation, and crystallographic reflections matching those of bone apatite (TEM-SAED),[30] corroborated by similar XRD patterns between synthetic scaffolds and compact bone.[80]

Small amounts of ions can sometimes have large effects of normal functioning of organs and tissues and on their repair and regeneration.[103,104] This is the concept behind the application of bioinorganics, which involves the use of (trace amounts of) ions to stimulate the regeneration of damaged tissue, much like a (organic) growth factor would do. This concept as well as various methods of incorporation of bioinorganics into, e.g., bone graft substitutes has been extensively discussed in several reviews.[102] It is therefore interesting to investigate whether bioinorganics can also be incorporated into the mineral deposited during intrafibrillar mineralization of collagen. This would not only make "closer-to-nature" materials, in terms of their chemical composition, but would also plausibly enhance their bone regenerative potential. Only a few examples exist of such studies, although some substitutions are to be expected due to the composition of the mineralization solution employed, containing carbonate, sodium, and potassium ions.

Characterization of the carbonate moiety by FTIR is typically done by deconvolution of the ν_2 CO_3^{2-} band between 850 and 890 cm^{-1} into three different peaks: at 866 cm^{-1} for unstable location, 871 cm^{-1} for B-substitution (PO_4^{3-} position), and 878 cm^{-1} for A-substitution (OH^- position).[105] Inductively coupled plasma optical emission spectroscopy (ICP-OES) or

mass spectrometry (ICP-MS) can provide good quantification of wt% of metallic ions, although by itself it is not sufficient to determine the exact position of the dopant, which can be incorporated into the crystalline lattice, adsorbed on the surface, or associated with the surrounding organic molecules. A complementary analysis by Rietveld refinement of diffraction data can substantiate evidence for the location of a substitute ion. This approach was used to characterize substitutions by Mn^{2+}, Co^{2+}, and Ni^{2+} in nanometer-sized citrate–carbonate–apatite (albeit in the absence of collagen, which could admittedly complicate the analysis), with good agreement between the theoretical pattern (calculated for a certain % of substitution in Ca^{2+}—data obtained by ICP-OES) and the experimental data.[106] Refinement of the diffraction data was also used for characterizing Mg^{2+}-substituted carbonated apatite and identifying preferential substitution in the Ca(II) position.[107] Other characterization methods to differentiate between adsorbed or lattice-incorporated dopants include ^{13}P, ^{1}H, or ^{43}Ca solid-state nuclear magnetic resonance spectroscopy (NMR), which can give information about the location of cation substitutions,[108–110] and small- and wide-angle X-ray scattering (SAXS and WAXS), which provides measurements of the lattice parameters, which are typically affected by substitutions from dopant ions with different radii. Additionally, SAXS/WAXS can also provide spatial resolution when used in the scanning mode.[111] Combination of electron microscopy with electron energy-loss spectroscopy (EELS) also offers chemical information with spatial resolution, as shown in a study where the formation of mineral deposits by mouse osteoblasts was observed to start from a CO_3^{2-}-rich ACP nodule.[60] Other useful methods of chemical mapping include time-of-flight secondary-ion mass spectrometry[112,113] and atom probe tomography.[114]

Although in general, the techniques that have been used for chemical and structural characterization of bone can also be applied to the intrafibrillar mineral produced in vitro, to the best of our knowledge, they have been used to a very limited extent in biomineralization studies. One study mentioned that the addition of strontium to the mineralization solution "strongly disrupted the [PILP] process," although no data were provided.[96] Strontium is known to decrease osteoclast-resorbing activity and differentiation, while promoting osteoblast differentiation,[115,116] which makes it attractive for bone regeneration strategies. Another study focused on the interference of copper that was included in the mineralization solution by dissolution from TEM grids. The ion was shown to completely prevent mineralization by the PILP process, by overstabilizing the ACP precursor, which was shown to infiltrate the collagen fibrils but remain amorphous for at least 72 h.[52] Copper is a known stimulator of angiogenesis,[117] which is of great value for large-defect regeneration.

Clearly, further research is necessary on the role of "foreign" ions in the polymer-induced mineralization process. It is important to understand whether they can be incorporated during the amorphous precursor formation phase or, as in the case of copper (and apparently strontium), they prevent the mineralization process altogether. This knowledge would not only increase our understanding of natural mineral formation, but could also aid the development of better performing bone graft substitutes.

2.3. Beyond Biomimetics: Replacing Collagen as the Structural Matrix for Biomineralization

Exploring synthetic biomaterials as a template for intrafibrillar-like mineralization can contribute to the development of novel bone graft substitutes that do not rely on collagen sources. In general, collagen used in these types of studies and developments is animal-derived, and finding synthetic alternatives paves the way toward more ethically responsible and sustainable strategies for bone regeneration. Another advantage of replacing collagen as the organic structural matrix is that by using a designed and more controlled system, it is possible to better understand the role of individual properties of both the structural template and the process-directing agent in the biomineralization process. Replicating the nanoscale organization of the organic–inorganic components of bone with synthetic materials is, however, not trivial because it is in part due to the collagen structure and composition that the organization of the apatite phase takes place, as pointed out by various studies.[55,56,66]

Nevertheless, a successful development was shown using the recombinant proteins elastin-like recombinamers (ELRs). These are recombinant proteins, inspired from a sequence derived from elastin, and capable of undergoing a soluble-insoluble transition at a critical temperature (termed inversed transition temperature T_t), aggregating in a stable conformation. For temperatures above T_t, ELRs were shown to undergo intrafibrillar-like mineralization (**Figure 3**). Characterization by TEM-SAED showed that the self-assembled and crosslinked ELR matrix was mineralized with randomly oriented, needle-like apatite crystals. X-ray diffraction confirmed the resemblance with bone apatite, and SEM-EDS showed maintenance of the hydrogel structural morphology and porosity despite extensive mineralization. Furthermore, mechanical characterization of the mineralized ELR was performed by nanoindentation both in dry and wet states, with bovine cortical bone used as control. The mineralized ELR had an elasticity modulus of 20.3 GPa, comparable to that of cortical bone with a modulus of elasticity being 25 GPa. The hardness of mineralized ELR matrix and cortical bone in the dry state was 0.93 and 1.2 GPa, respectively. In the wet state, the mechanical properties of mineralized ELR were about one-third of those of cortical bone.[118]

A subsequent study by the same group gave evidence that the spaces created within ELR fibrils were responsible for its infiltration with the ACP precursor, and subsequent intrafibrillar mineralization. By using pAsp or PAH as process-directing agents that create, respectively, negative and positive charged ACP–polymer complexes, mineralization of the positively charged ELR (due to lysine residues) occurred in both cases. This suggests that electrostatic interactions are not the driving force behind the infiltration of an amorphous phase, as mentioned in other studies.[56] It was also observed that the ELRs containing bioactive sequences formed gels that were less stable than the gels formed by ELRs containing the backbone sequence alone. It was hypothesized that the bioactive sequences disrupted the otherwise stable secondary structures—β-spirals—that form at temperatures higher than T_t. However, mineral was reported to be found within the fibrils of all ELRs.

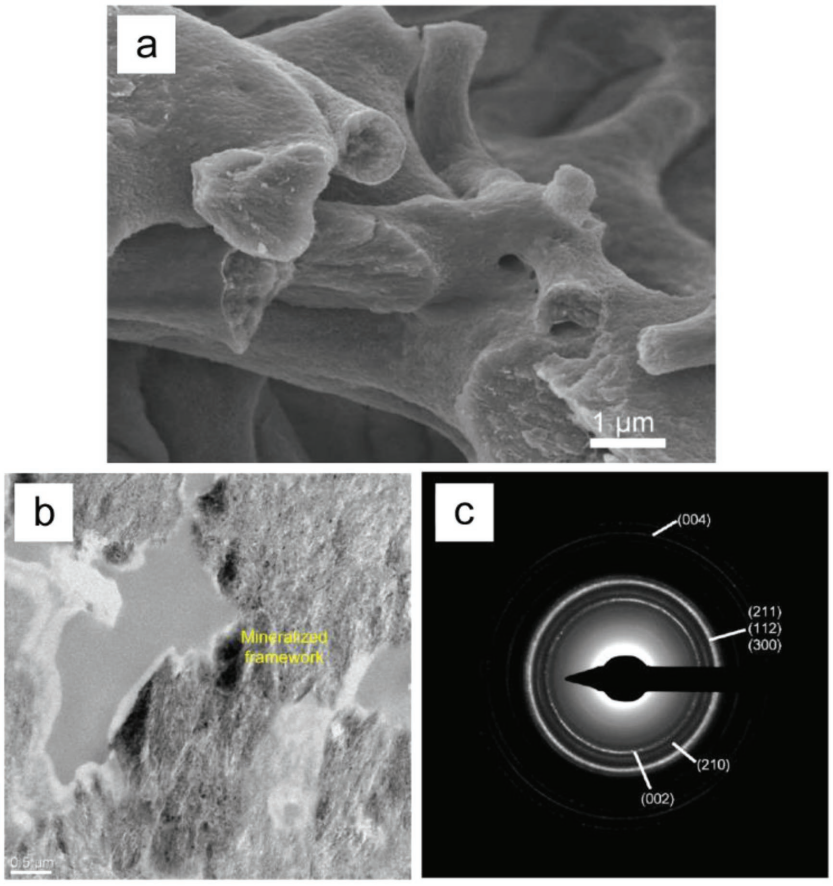

Figure 3. Intrafibrillar mineralization of an ELR sponge. a) SEM image of an ELR sponge mineralized for 7 days, b) bright field TEM image of an ELR fiber mineralized for 14 days, and c) corresponding SAED pattern showing relatively random distribution of the *c*-axis components 002 and 004, as well as reflections from the 211, 112, 300, and 210 planes. Reproduced with permission.[118] Copyright 2015, American Chemical Society.

The specific advantages of the ELR system stem from their recombinant nature. The ability to engineer specific peptide sequences allows controlled design of, for example, self-assembly properties, mechanical stability, or inclusion of bioactive sequences.[119] The drawback with recombinant peptides is their cost, which currently poses a barrier to upscaling.

2.4. Scaling Up: From a Building Block to 2D and 3D Constructs

Organization of the building blocks into structures with different hierarchical levels is the next step in constructing a bone mimicking biomaterial/bone graft substitute. Referring to bone structure, fiber bundles and lamellae are the structures that are next on the length scale following single fibrils. At the 1–10 µm range, the emergent characteristic of fibril organization is the parallel array of fiber bundles.

Reconstituted fibrils from diluted acidic solutions generally have a random orientation. Many different attempts have been undertaken to align the fibrils along a given direction, and more in general, to structure collagen scaffolds.[120] The approaches we will discuss here are not exhaustive; they were selected only if the following three conditions were fulfilled: 1) the capacity to produce collagen fibrils that retain the periodic *D*-spacing; 2) the ability to form 2D or 3D structures that are relevant from a bone-mimicking perspective; and 3) the applicability to either in vitro cell models or potential for upscaling to larger, implantable constructs.

Electrochemically aligned collagen fibrils can be produced by generating an electric potential difference across a dialyzed collagen solution. Using this method, fibril bundles were produced ranging from tens to hundreds of micrometers in thickness, and centimeters in length. Tropocollagen molecules align in a medium that is far from ideal for fibrillogenesis: they are at their isoelectric point (no charged residues) and there is close to zero ionic strength, due to the dialysis step. Subsequent incubation in phosphate-buffered saline is critical for allowing proper fibril formation. The process can be complemented with crosslinking. Although the characteristic *D*-spacing pattern could not be confirmed by SEM or TEM, the SAXS pattern showed similarity with that of a natural tendon. While this method is promising for the production of large and oriented collagen structures, more data is needed on the conservation of the native fibril conformation.[121,122]

A combination of wet spinning, fibrillogenesis step, and subsequent application of uniaxial strain (15% or 30%) produced highly aligned, elliptical-shaped fibrils, with the cross-sectional dimensions of about 50×20 µm. *D*-spacing of the fibrils was confirmed by TEM, although some unbanded parts were still present (**Figure 4**). This method was used to produce fibers that were hundreds of meters long.[123] Wet spinning uses a combination of solvents that is typically not compatible with the self-assembly of tropocollagen into native quarter-staggered conformation, so a second incubation step is necessary, where the drawn "amorphous" collagen fiber is immersed in a fibril formation buffer, e.g., PBS. The impact of the spinning process on the capacity of the tropocollagen molecules to assemble within the already drawn fiber is not clear, and more studies are needed to characterize the fibrillogenesis process after wet spinning. Nonetheless, this method shows great promise for scaling up: from drawn fibers of collagen into 2D sheets with control over fiber orientation, for example, by using weaving techniques and potentially into 3D scaffolds.[124,125]

Magnetic fields have also been used for aligning collagen gels, as the tropocollagen molecule has a permanent dipole, as does the aggregated fibril. A strong magnetic field (12 T) was applied to a 5 mm thick collagen gel (9 mg mL^{-1}) for 3 h, resulting in alignment of about 85% of the fibers within 10° of the expected direction, as was shown by the SEM microscopic images.[126] While these microscopic images only

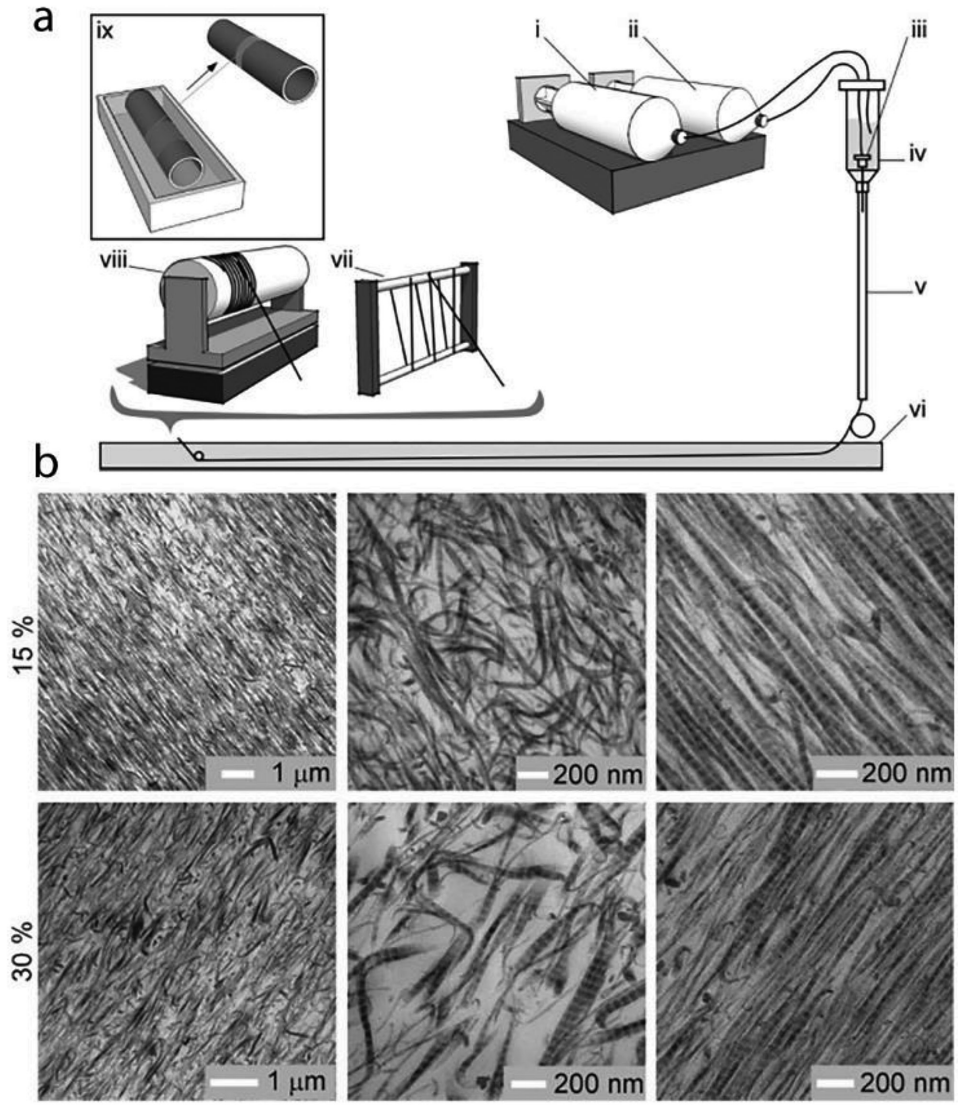

Figure 4. Wet spinning for collagen fibril alignment. a) Schematic of the wet spinning setup, showing syringes i,ii) with collagen and buffer solutions that are injected into a needle iii), housed in a bubble trap iv), with a glass capillary v) leading to a bath containing the fiber formation buffer vi); fibers are collected manually vii) or automatically in a spool viii), and finally go through a 70% ethanol bath before being air dried ix); b) bright field TEM of sections of collagen fibers stained with 2% uranyl acetate after being subjected to 15% or 30% strain. While low-magnification images (left column) show highly aligned fibers, close inspection reveals in both cases areas of disorder (middle column) and order (right column) within the same fiber. Reproduced with permission.[123] Copyright 2009, Wiley Periodicals.

showed the gel surface, it would be interesting to investigate the alignment of the fibers in the bulk of the thick gels. Formation of fibrils with periodic *D*-spacing was not disturbed by the magnetic field, as shown by SEM[127] and AFM.[126] Weaker magnetic fields were also able to induce alignment of fibrils, provided that magnetic particles (e.g., iron oxide nanoparticles) were embedded in the collagen matrix.[128,129] However, the presence of these extra particles could hamper the mineralization process.

Using a soft lithography method microtransfer molding (μTM), Naik et al. were able to produce collagen patterns on flat surfaces, although with little evidence about their native conformation.[130] Also several microfluidic-based methods were used for producing aligned collagen fibrils. A flow-assisted patterning method using parallel microchannels was used to deposit aligned fibrils. It was shown that smaller channel width led to increasing frequency of alignment, with 10 μm wide channels having about 40% fibers within 5° of the channel direction.[131] These strategies, although useful for producing 2D substrates for studies on cell–material interaction, have limited potential for upscaling into 3D structures. A study using hydrodynamic focusing showed a great potential for continuous production of a collagen fiber of controllable width, in a manner similar to wet spinning, but with overall smaller fiber diameters and more control over the diameter (**Figure 5**).[132] Although the conditions of fibrillogenesis in these studies are amenable to formation of the native *D*-spacing, the data proving this were largely absent in these studies.

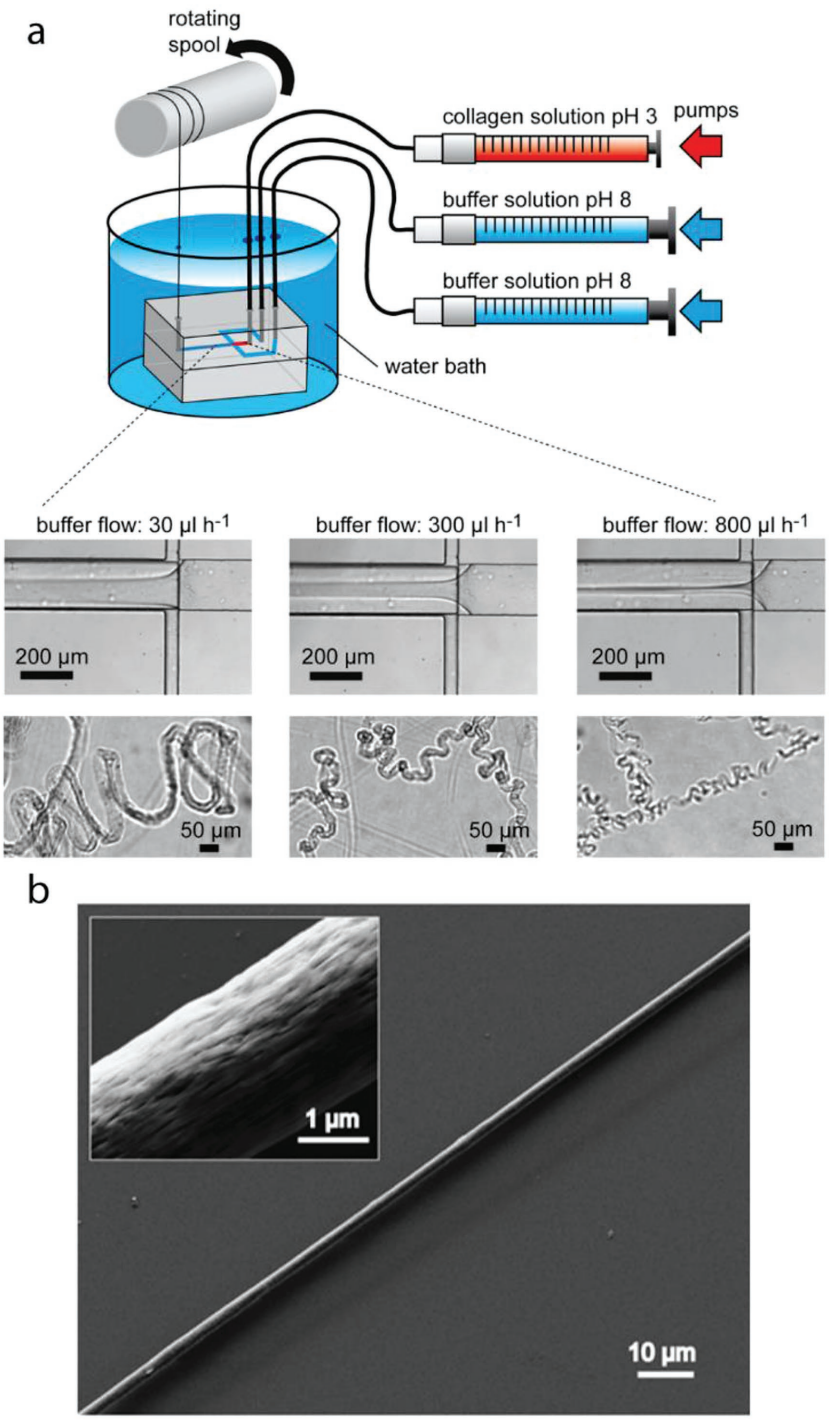

Figure 5. Microfluidic extrusion of collagen fibrils by hydrodynamic focusing. a) Schematic of the setup, with two inlets for buffer solution (blue) and one for the collagen solution (red); the microfluidic chip is housed inside a beaker with fiber formation buffer, where the fiber passes through while being collected by a spool. This technique allows great control over fiber diameter, as seen in the images of different fiber diameter produced at different flow rates. b) SEM image of a collagen fibril produced using this system. Reproduced with permission.[132] Copyright 2016, American Chemical Society.

Apart from fibril orientation, another important characteristic for production of 2D or 3D collagen constructs is the packing of collagen molecules, and the density of the final material. Again, referring to the composition of natural bone, a biomimicking material should contain ≈65 wt% apatite, 25 wt% organic matter and a maximum of about 10 wt% water. Some examples of intrafibrillar mineralization studies presented in the previous section reported mineral content, as determined by TGA, of around 65 wt%.[77,80] However, as most samples are lyophilized before the analysis, the reported weight percentages are those of the dry substrate.

This value is often compared directly with the inorganic content of bone cited in the literature, of 65 wt%, without mention of the water content in the scaffold. It should be noted that the 65 wt% pertains to wet bone, and that the corresponding weight percentage of inorganic content in a dry sample would is about 72 wt%. So if a mineralized and lyophilized collagen scaffold shows 65 wt% inorganic content, this is still very comparable to the 72 wt% found in bone. This means that the *collagen fibrils* (and not the scaffold as a whole) have a mineral content that is indeed close to that of bone fibrils. Indeed, the in vitro-prepared substrates have higher porosity and take up much more than the 10 wt% water that bone usually contains. This becomes apparent when the mechanical properties of the biomineralized materials are measured in the wet state. Under wet conditions, the elastic modulus and hardness are generally much lower than what would be expected if the water content of such a material would be similar to that of bone.[80] The concentrations of commercially available acidic solutions of collagen range from 2 to 10 mg mL^{-1}, which is 25–125 times lower than in natural bone. This means that in order to have a substrate with around 10 wt% of water, common collagen solutions or gels have to be concentrated. A few approaches to produce dense matrices from diluted solutions of collagen have been described.

For example, based on reports that collagen exhibits a behavior similar to liquid crystals at high concentrations (>80 mg mL^{-1}), assembling into a cholesteric structure in vitro that is reminiscent of the angular step between adjacent lamella,[133,134] Wang et al. produced organized and dense matrices from a diluted collagen solution, via a combination of injection and reverse dialysis.[135] TEM and SEM microscopic images of these dense scaffolds showed features with some similarity to osteonal bone, while collagen fibrils showed the characteristic *D*-spacing, confirming that they were well formed.

Due to the method used, with injection (8 days), dialysis (4 days), and fibrillogenesis (4 days), the entire process was lengthy, compounded with 16 additional days to achieve 50 wt% mineral content. Nevertheless, a dense scaffold was formed, showing a degree of organization that bears some resemblance to osteonal bone, which is a notable achievement.

Extensive and homogeneous mineralization of large, dense scaffolds remains a challenge, as was also illustrated by the relatively limited infiltration depth of PILP precursors in demineralized bone (up to 100 μm)[69] and tendon tissue (up to 500 μm).[76]

An alternative method to obtain dense collagen scaffolds in vitro is by applying compression to typical collagen gel formulations, increasing their concentration by forcing out the water.[136,137] This approach was used by Li et al. to obtain dense collagen matrices, in the form of a 100 μm thick membrane with collagen concentration of around 80 mg mL^{-1}.[80] Homogenous mineralization by the PILP method was confirmed by SEM-EDS analysis of a cross-section of the membrane. This method yielded randomly oriented fibrils and a substrate that was less dense than the ones produced by the injection-dialysis method described above. After crosslinking and mineralization (64 wt% dry weight), the membrane had an elastic modulus of 9 GPa and hardness of 0.7 GPa, which were about one third of the values for lamellar bone in the dry state. When measured in the wet state, the mechanical properties decreased even further, reaching the elastic modulus of around 0.2 GPa, close to that of woven bone in the wet state. This comparison shows that, in order to mimic the mechanical properties of bone, further compaction of the collagen matrix, in combination with successful mineralization, is necessary.

Design of osteon-like structures that replicate its level of hierarchical organization is a difficult task to undertake. Current 3D printing techniques focus on the reconstruction of the central Haversian canal and network of micro channels surrounding it, typically using a biocompatible polymer like poly(lactic acid).[138] Printing techniques, however, are not capable of achieving high collagen density. An alternative approach could include a reverse-dialysis or compression method on a collagen gel containing a sacrificial framework that would be washed away in a subsequent step, creating a network of interconnected channels within a dense scaffold.

2.5. Evaluation of Bioactivity

An important step in research and development of biomaterials for bone regeneration is the investigation of their interactions with relevant cells in vitro, such as osteoblasts, mesenchymal stem cells, etc., as a means to evaluate their bioactivity. Interestingly, only a limited number of studies exist in which collagen substrates with intrafibrillar mineralization were evaluated in vitro using cell culture systems.

In one of these studies, a crosslinked and phosphorylated collagen gel was formed on coverslips and mineralized using an SBF-like solution containing PAA. This substrate was used for culturing human periodontal ligament stem cells up to 21 days, in culture medium without stimulators of osteogenic differentiation. Controls included a collagen scaffold mineralized in the same SBF-like solution, but without PAA, as well as unmineralized collagen. Quantification of osteogenic gene expression showed upregulation of OPN, COL1A1, and BMP2 mRNA on the intrafibrillar mineralized collagen as compared to the controls. Moreover, alizarin red staining showed more pronounced mineralization on the scaffolds with intrafibrillar mineralization.[139]

In another study, an intrafibrillar-mineralized collagen scaffold was prepared using phosphorylated collagen and PAA, followed by the 21 day culture of human umbilical cord mesenchymal stem cells. Controls included collagen mineralized in the absence of PAA, nonphosphorylated mineralized collagen and unmineralized collagen. ALP activity of the cells cultured on intrafibrillar-mineralized collagen scaffold was higher than on the controls only after 21 days, while no differences were observed at earlier time points. These constructs were also implanted in a femoral bone defect model in rabbits. Complete defect healing after 12 weeks was only shown for the intrafibrillar-mineralized collagen, by the MRI and micro-CT analyses.[140]

A collagen scaffold with intrafibrillar mineralization, prepared with carboxymethyl chitosan as process-directing agent, was used for culturing mouse MC3T3-E1 osteoblast-like cells, for 7 days. An SBF-mineralized collagen scaffold and a collagen-only scaffold served as controls. ALP activity was higher for the scaffold with intrafibrillar mineralization after 5 and 7 days, although not at the earliest time point. These constructs were also implanted in a cranial defect model in rats, where only the intrafibrillar-mineralized scaffold showed almost complete defect closure within 8 weeks, as demonstrated by μCT and histological data.[141]

In an elegant study by Jiao et al., a biphasic silica/apatite mineralized collagen scaffold was prepared by a two-step PILP-like procedure, where PAH was used for stabilization of the silica-containing medium, and pAsp for the CaP-containing medium. Controls included a silicified-collagen substrate, a calcified-collagen substrate, and a collagen-only substrate. The in vitro cell culture was performed using mouse mesenchymal stem cells, as well as mouse macrophage cell line RAW264.7, capable of undergoing differentiation toward osteoclasts. The differentiation of mMSC in osteogenic medium, assessed by the ALP activity, was highest on the biphasic scaffold. Quantitative real-time polymerase chain reaction showed a strong effect of silica incorporation: upregulation of ALP, OPN, and OPG on the one hand, and downregulation of osteoclast-activating RANKL on the other, for the biphasic and silica–collagen scaffolds. When biphasic and silica–collagen scaffolds were compared, a higher expression of the osteogenic markers was observed on the former type. The OPG upregulation and RANKL downregulation were confirmed by the Western blot analysis. Furthermore, in a coculture of RAW264.7 cells with scaffold-conditioned mMSC, it was shown that the number of TRAP-positive cells and area of resorption pits were decreased for conditions where the mMSC were cultured on silicified and biphasic scaffolds. The authors further completed the study by uncovering the signaling pathways behind the observed mechanism of inhibition of osteoclastogenesis through a series of pathway-inhibition experiments.[93]

Another study used OPN- or pAsp-assisted mineralization of demineralized slices of bovine femur, and compared the influence of the process-directing agent on mouse osteoclasts

derived from bone marrow. Controls were unaltered bone slices, as well as demineralized slices that were remineralized in the absence of OPN or pAsp. Immunofluorescence and SEM results showed, respectively, that the number of actin rings and resorption pits formed were lower on the pAsp-remineralized slices than on the unaltered bone slices. In contrast, the number of actin rings and resorption pits was higher when the slices were remineralized by OPN.[53] These results suggest that OPN has a role in cell-mediated bone resorption, corroborated with evidence for less resorption by OPN-deficient mice.[142,143]

Although limited in number, the available studies on the in vitro bioactivity of intrafibrillar-mineralized collagen scaffolds show promising results, both in terms of support of differentiation of multipotent stem cells toward the osteogenic lineage, as well as for being able to be resorbed by cell-mediated phenomena. The two in vivo experiments[140,141] reviewed also show promising results, with better healing of bone defects when compared to the respective controls.

Continued biological experiments to evaluate the bioactivity of bone-mimicking substitutes are a necessity, to validate material design and investigate whether pursuit of the biomimetic route indeed delivers on its promises.

2.6. Translation to the Clinic

Some efforts have been made to translate the amorphous precursor systems into clinical strategies for remineralization of hypo-mineralized tissues, as solution-based systems have limitations for application in a clinical situation. Typically these efforts involve the use of a carrier system to deliver the mineralizing components to the target tissue. For example, mesoporous silica nanoparticles were loaded with PAA-stabilized ACP, and used for mineralizing reconstituted collagen fibrils in vitro. TEM analysis showed the presence of intrafibrillar mineral, throughout the collagen network, after 4 days.[144,145]

Another example is the use of self-etch adhesives, currently used in the treatment of dental cavities, as a carrier system for pAsp-stabilized silica-doped ACP. When tested on demineralized dentin, the adhesives produced a 1–2 μm layer of lightly remineralized tissue after 14 days, close to the native dentin.[146]

These examples show a simple and effective way of translating an in vitro concept of biomineralization directly to a clinical setting, and are a promising first step toward developing biomimetic remineralization systems. The current challenges are related to volume of mineralizing components that can be delivered; the adhesive mentioned above was loaded with 25 wt% of amorphous precursor particles, which could potentially be increased, but not by a large amount. Alternative strategies could focus on using the mineral ions present in surrounding physiological fluids as the source for continued mineralization.

3. Conclusion and Outlook

Successful intrafibrillar mineralization of collagen substrates in vitro, achieved in the past decade, has been an important step forward toward truly biomimetic bone-like structures. As is evident from the different studies reviewed here, the lab-made building blocks closely replicate some of the most important features found natural tissue, such as mineral density, particle size, and crystallite orientation. Nevertheless, for some other characteristics, it is still unclear to which extent the in vitro built structures resemble their natural counterparts. For example, more characterization of the chemical identity of the in vitro formed intrafibrillar mineral is required, in particular regarding the substitutions by ions present in the mineralizing solution. This could deliver further insights into the mechanism of polymer-assisted mineralization as some ions were shown to disrupt the process. Furthermore, while present in low (often trace) amounts in natural bone mineral, the relevance of these ions should not be ignored; on the contrary, bioinorganic additives to the mineral may enhance the bone regenerative potential to the biomimetic bone graft substitutes.

This review has also shown the importance of advanced analytical techniques in understanding the natural process of biomineralization, which in turn should be applied to the design and development of new biomimetic biomaterials. For example, the curved needle–like crystallites, shown by 3D reconstruction of HR-TEM of bone slices to interpenetrate more than one collagen fibril,[31] put in question the division between intrafibrillar and extrafibrillar mineral and beg for new hypothesizes regarding the formation of these structures. Furthermore, continued research toward full understanding of the roles of NCPs in bone mineralization might shed light upon the crystallization process of these particles.

Research into and development of (synthetic) alternatives to collagen as structural component of the ECM is also highly important for two reasons. First, the use of synthetic, often well-characterized materials may contribute to the knowledge of the fundamentals of biomineralization, for example, regarding the role of NCPs, by allowing a direct comparison with collagen. Second, the development of collagen alternatives is highly important from a translational perspective, where the use of a synthetic material has several advantages over the (xenogeneic) collagen. The only system that has shown convincing intrafibrillar-like mineralization is based on recombinant proteins, which add versatility and customization features, but are expensive for upscaling. Therefore, efforts to develop other alternative matrices that can overcome this issue are justified. As exemplified by the ELRs, and also by a study on mineralization upon physical confinement,[147] a critical feature for intrafibrillar-like mineralization seems to be the existence of stable, structural confined spaces. This is achieved in both collagen and ELR by the assembly of small building blocks, of tropocollagen and β-spirals, respectively, into larger hierarchical structures—collagen fibrils (staggered tropocollagen molecules) and ELR filaments (association of folded β-spirals). It is envisioned that by this same principle of producing stable molecular structures with nanoporosity, other polymeric systems can be used for intrafibrillar-like mineralization.

Upscaling from a building block into organized 2D and 3D assemblies comes with two main challenges: directionality of the collagen fibers and compact arrangement into dense substrates.

State-of-the-art methodologies capable of aligning collagen fibrils while retaining their capacity for bone-like mineralization come from many different fields. Of note are wet

spinning[123] and microfluidic[132] approaches that have the potential to produce aligned bundles of fibers with the native *D*-spacing, as well as the advantage of having some control over fiber diameter.

These can be combined with other techniques, for example weaving of biopolymers,[125] to fabricate 2D bidirectional meshes of parallel collagen fibers. Control over the fibril thickness and pore dimension, and further stacking of 2D meshes would result in a 3D structure structurally resembling cancellous bone.

It should be emphasized that one of the main reasons for pursuing the biomimetic approaches to develop synthetic bone graft substitutes is the potential to match the mechanical characteristics of natural bone, which cannot be achieved with currently widely used (CaP) ceramic bone graft substitutes, which are intrinsically brittle. Interestingly, in many studies reviewed here, the mechanical properties have not been extensively evaluated, while specific mechanical tests would be useful, for example, in determining the importance of fibril alignment.

It has been shown that the elastic modulus of synthetic scaffolds is about 33% (for ELR) and 13% (for collagen) of that of lamellar bone. This difference can be attributed to an insufficient fibril density of the synthetic scaffolds, which generally perform poorly when in the wet state. Replication of the cortical bone density requires the mineralization of large collagen substrates with limited porosity (≈6%), which is a challenging task. The study by Wang et al. is a good example of exploiting the liquid-crystal behavior of collagen solutions, at high concentrations, to form dense collagen substrates that also show some degree of fiber orientation.[66] Another promising method is the use of plastic compression applied to gels with prealigned fibrils, obtained, for example, using magnetic fields.

While 3D constructs are essential from a translational/clinical perspective, planar structures are a necessary step in getting there, meanwhile being useful for cell–material interaction studies that provide data to sustain further developments of biomimetic materials. As discussed in the last section of the review, the number of studies dealing with the interactions between relevant cells and the latest wave of biomimetic materials for bone regeneration is limited. Nevertheless, the results of these studies are compelling. In particular, further studies concentrating on the interplay between osteoblasts and osteoclasts would be useful in establishing a model for resorption and replacement of these synthetic substrates by natural bone ECM.

It must be noted that the reason for choosing a biomimetic route to biomaterial design and development does not come solely from its potential to deliver better materials for the clinic. Indeed, no consensus in the field of materials for biomedical applications exists that biomimetic or bioinspired methods are more promising than other methods for developing successful treatments of damaged and diseased organs and tissues. Nevertheless, by using more natural-like strategies in vitro, it is sometimes possible to link laboratory evidence to actual in vivo mechanisms, as was the case for the discovery of amorphous precursors in vertebrate bone. The combination of fundamental and applied studies that take place at the biomimetic border fuels each other into new discoveries, and this is one of the main strengths of biomimetism.

Acknowledgements

This research has been made possible with the support of the Dutch Province of Limburg.

Conflict of Interest

The authors declare no conflict of interest.

Keywords

biomaterials, biomineralization, bones, intrafibrillar mineralization, regeneration

Received: June 18, 2018
Revised: August 23, 2018
Published online: September 21, 2018

[1] V. Campana, G. Milano, E. Pagano, M. Barba, C. Cicione, G. Salonna, W. Lattanzi, G. Logroscino, *J. Mater. Sci.: Mater. Med.* **2014**, *25*, 2445.
[2] S. N. Khan, F. P. Cammisa, H. S. Sandhu, A. D. Diwan, F. P. Girardi, J. M. Lane, *J. Am. Acad. Orthop. Surg.* **2005**, *13*, 77.
[3] R. Dimitriou, G. I. Mataliotakis, A. G. Angoules, N. K. Kanakaris, P. V. Giannoudis, *Injury* **2011**, *42*, S3.
[4] T. Kurien, R. G. Pearson, B. E. Scammell, *Bone Jt. J.* **2013**, *95B*, 583.
[5] D. Salem, Z. Natto, S. Elangovan, N. Karimbux, *J. Periodontol.* **2016**, *87*, 872.
[6] J.-H. Zeng, S.-W. Liu, L. Xiong, P. Qiu, L.-H. Ding, S.-L. Xiong, J.-T. Li, X.-G. Liao, Z.-M. Tang, *J. Orthop. Surg. Res.* **2018**, *13*, 33.
[7] D. Rickert, J. J. R. H. Slater, H. J. A. Meijer, A. Vissink, G. M. Raghoebar, *Int. J. Oral Maxillofac. Surg.* **2012**, *41*, 160.
[8] R. Agarwal, K. Williams, C. A. Umscheid, W. C. Welch, *J. Neurosurg. Spine* **2009**, *11*, 729.
[9] D. M. Fisher, J. M.-L. Wong, C. Crowley, W. S. Khan, *Curr. Stem Cell Res. Ther.* **2013**, *8*, 260.
[10] A. Moya, J. Paquet, M. Deschepper, N. Larochette, K. Oudina, C. Denoeud, M. Bensidhoum, D. Logeart-Avramoglou, H. Petite, *Stem Cells* **2018**, *36*, 363.
[11] W. Wang, K. W. K. Yeung, *Bioact. Mater.* **2017**, *2*, 224.
[12] A. W. Ritting, E. W. Weber, M. C. Lee, *J. Hand Surg. Am.* **2012**, *37*, 316.
[13] S. Boraiah, O. Paul, D. Hawkes, M. Wickham, D. G. Lorich, *Clin. Orthop. Relat. Res.* **2009**, *467*, 3257.
[14] H. S. Johal, R. E. Buckley, I. L. D. Le, R. K. Leighton, *J. Trauma Acute Care Surg.* **2009**, *67*, 875.
[15] T. A. Russell, R. K. Leighton, *J. Bone Jt. Surg.* **2008**, *90*, 2057.
[16] H. Bae, H. P. J. Hatten, R. Linovitz, A. D. Tahernia, M. K. Schaufele, V. McCollom, L. Gilula, P. Maurer, R. Benyamin, J. M. Mathis, M. Persenaire, *Spine* **2012**, *37*, 544.
[17] T. Lerner, V. Bullmann, T. L. Schulte, M. Schneider, U. Liljenqvist, *Eur. Spine J.* **2009**, *18*, 170.
[18] C. Cassidy, J. B. Jupiter, M. Cohen, M. Delli-Santi, C. Fennell, C. Leinberry, J. Husband, A. Ladd, W. R. Seitz, B. Constanz, *J. Bone Joint Surg. Am.* **2003**, *85-A*, 2127.
[19] M. Bohner, L. Galea, N. Doebelin, *J. Eur. Ceram. Soc.* **2012**, *32*, 2663.
[20] M. Granke, M. D. Does, J. S. Nyman, *Calcif. Tissue Int.* **2015**, *97*, 292.
[21] P. Fratzl, R. Weinkamer, *Prog. Mater. Sci.* **2007**, *52*, 1263.
[22] S. P. Robins, J. D. Brady, in *Principles of Bone Biology*, Vol. *1* (Eds: J. P. Bilezikian, L. G. Raisz, T. J. Martin), Academic Press, MA **2008**, Ch. 16.

[23] M. Saito, K. Marumo, *Calcif. Tissue Int.* **2015**, *97*, 242.
[24] J. R. Harris, A. Soliakov, R. J. Lewis, *Micron* **2013**, *49*, 60.
[25] W. Zhu, P. G. Robey, A. L. Boskey, in *Osteoporosis*, Vol. *1* (Eds: R. Marcus, D. Feldman, D. Nelson, C. Rosen), Academic Press, MA **2008**, Ch. 9.
[26] P. J. Thurner, C. G. Chen, S. Ionova-Martin, L. Sun, A. Harman, A. Porter, J. W. Ager, R. O. Ritchie, T. Alliston, *Bone* **2010**, *46*, 1564.
[27] A. A. Poundarik, T. Diab, G. E. Sroga, A. Ural, A. L. Boskey, C. M. Gundberg, D. Vashishth, *Proc. Natl. Acad. Sci. USA* **2012**, *109*, 19178.
[28] E. A. McNally, H. P. Schwarcz, G. A. Botton, A. L. Arsenault, *PLoS One* **2012**, *7*, e29258.
[29] E. McNally, F. Nan, G. A. Botton, H. P. Schwarcz, *Micron* **2013**, *49*, 46.
[30] M. J. Olszta, X. Cheng, S. S. Jee, R. Kumar, Y. Y. Kim, M. J. Kaufman, E. P. Douglas, L. B. Gower, *Mater. Sci. Eng., R* **2007**, *58*, 77.
[31] N. Reznikov, M. Bilton, L. Lari, M. M. Stevens, R. Kröger, *Science* **2018**, *360*, eaao2189.
[32] B. Wopenka, J. D. Pasteris, *Mater. Sci. Eng., C* **2005**, *25*, 131.
[33] R. K. Rude, in *Principles of Bone Biology*, Vol. *1* (Eds: J. P. Bilezikian, L. G. Raisz, T. J. Martin), Academic Press, MA **2008**, Ch. 24.
[34] E. Boanini, M. Gazzano, A. Bigi, *Acta Biomater.* **2010**, *6*, 1882.
[35] F. Bronner, in *Principles of Bone Biology*, Vol. *1* (Eds: J. P. Bilezikian, L. G. Raisz, T. J. Martin), Academic Press, MA **2008**, Ch. 25.
[36] O. A. Golovanova, N. N. Strunina, S. A. Lemesheva, B. T. Baisova, *J. Appl. Spectrosc.* **2011**, *78*, 145.
[37] N. P. Zaksas, T. T. Sultangazieva, V. A. Gerasimov, *Anal. Bioanal. Chem.* **2008**, *391*, 687.
[38] G. Ma, X. Y. Liu, *Cryst. Growth Des.* **2009**, *9*, 2991.
[39] L. C. Costello, M. Chellaiah, J. Zou, R. B. Franklin, M. A. Reynolds, *J. Regener. Med. Tissue Eng.* **2014**, *3*, 4.
[40] Y.-Y. Hu, A. Rawal, K. Schmidt-Rohr, *Proc. Natl. Acad. Sci. USA* **2010**, *107*, 22425.
[41] E. Davies, K. H. Muller, W. C. Wong, C. J. Pickard, D. G. Reid, J. N. Skepper, M. J. Duer, *Proc. Natl. Acad. Sci. USA* **2014**, *111*, E1354.
[42] J. M. Delgado-López, F. Bertolotti, J. Lyngsø, J. S. Pedersen, A. Cervellino, N. Masciocchi, A. Guagliardi, *Acta Biomater.* **2017**, *49*, 555.
[43] J. Mahamid, A. Sharir, L. Addadi, S. Weiner, *Proc. Natl. Acad. Sci. USA* **2008**, *105*, 12748.
[44] M. Bennet, A. Akiva, D. Faivre, G. Malkinson, K. Yaniv, S. Abdelilah-Seyfried, P. Fratzl, A. Masic, *Biophys. J.* **2014**, *106*, L17.
[45] J. Mahamid, B. Aichmayer, E. Shimoni, R. Ziblat, C. Li, S. Siegel, O. Paris, P. Fratzl, S. Weiner, L. Addadi, *Proc. Natl. Acad. Sci. USA* **2010**, *107*, 6316.
[46] J. Mahamid, A. Sharir, D. Gur, E. Zelzer, L. Addadi, S. Weiner, *J. Struct. Biol.* **2011**, *174*, 527.
[47] N. J. Crane, V. Popescu, M. D. Morris, P. Steenhuis, M. A. Ignelzi, *Bone* **2006**, *39*, 434.
[48] E. Beniash, R. A. Metzler, R. S. K. Lam, P. U. P. A. Gilbert, *J. Struct. Biol.* **2009**, *166*, 133.
[49] J. J. De Yoreo, P. U. P. A. Gilbert, N. A. J. M. Sommerdijk, R. L. Penn, S. Whitelam, D. Joester, H. Zhang, J. D. Rimer, A. Navrotsky, J. F. Banfield, A. F. William, F. M. Michel, F. C. Meldrum, H. Cölfen, P. M. Dove, *Science* **2015**, *349*, aaa6760.
[50] W. J. E. M. Habraken, J. Tao, L. J. Brylka, H. Friedrich, L. Bertinetti, A. S. Schenk, A. Verch, V. Dmitrovic, P. H. H. Bomans, P. M. Frederik, J. Laven, P. van der Schoot, B. Aichmayer, G. de With, J. J. De Yoreo, N. Sommerdijk, *Nat. Commun.* **2013**, *4*, 1507.
[51] A. S. Deshpande, P. A. Fang, X. Zhang, T. Jayaraman, C. Sfeir, E. Beniash, *Biomacromolecules* **2011**, *12*, 2933.
[52] F. Nudelman, P. H. H. Bomans, A. George, G. de With, N. A. J. M. Sommerdijk, *Faraday Discuss.* **2012**, *159*, 357.
[53] D. E. Rodriguez, T. Thula-Mata, E. J. Toro, Y. W. Yeh, C. Holt, L. S. Holliday, L. B. Gower, *Acta Biomater.* **2014**, *10*, 494.
[54] D. Toroian, E. L. Joo, P. A. Price, *J. Biol. Chem.* **2007**, *282*, 22437.
[55] P. A. Price, D. Toroian, J. E. Lim, *J. Biol. Chem.* **2009**, *284*, 17092.
[56] F. Nudelman, K. Pieterse, A. George, P. H. H. Bomans, H. Friedrich, L. J. Brylka, P. A. J. Hilbers, G. De With, N. A. J. M. Sommerdijk, *Nat. Mater.* **2010**, *9*, 1004.
[57] A. J. Lausch, E. D. Sone, *Biomacromolecules* **2015**, *16*, 1938.
[58] W. E. G. Müller, H. C. Schröder, U. Schlossmacher, V. A. Grebenjuk, H. Ushijima, X. Wang, *Biomaterials* **2013**, *34*, 8671.
[59] X. Wang, H. C. Schröder, U. Schlossmacher, M. Neufurth, Q. Feng, B. Diehl-Seifert, W. E. G. Müller, *Calcif. Tissue Int.* **2014**, *94*, 495.
[60] K. Nitiputri, Q. M. Ramasse, H. Autefage, C. M. McGilvery, S. Boonrungsiman, N. D. Evans, M. M. Stevens, A. E. Porter, *ACS Nano* **2016**, *10*, 6826.
[61] K. Jiao, L. Niu, C. F. Ma, X. Q. Huang, D. D. Pei, T. Luo, Q. Huang, J. H. Chen, F. R. Tay, *Adv. Funct. Mater.* **2016**, *26*, 6858.
[62] J. Mitchell, A. H. van Heteren, *C. R. Palevol* **2016**, *15*, 23.
[63] T. G. Bromage, H. M. Goldman, S. C. McFarlin, J. Warshaw, A. Boyde, C. M. Riggs, *Anat. Rec.* **2003**, *274B*, 157.
[64] T. Yamamoto, T. Hasegawa, M. Sasaki, H. Hongo, C. Tabata, Z. Liu, M. Li, N. Amizuka, *J. Electron Microsc.* **2012**, *61*, 113.
[65] L. B. Gower, D. J. Odom, *J. Cryst. Growth* **2000**, *210*, 719.
[66] Y. Wang, T. Azaïs, M. Robin, A. Vallée, C. Catania, P. Legriel, G. Pehau-Arnaudet, F. Babonneau, M. M. Giraud-Guille, N. Nassif, *Nat. Mater.* **2012**, *11*, 724.
[67] A. Akiva, G. Malkinson, A. Masic, M. Kerschnitzki, M. Bennet, P. Fratzl, L. Addadi, S. Weiner, K. Yaniv, *Bone* **2015**, *75*, 192.
[68] D. Kim, B. Lee, S. Thomopoulos, Y.-S. Jun, *Cryst. Growth Des.* **2016**, *16*, 5359.
[69] T. T. Thula, D. E. Rodriguez, M. H. Lee, L. Pendi, J. Podschun, L. B. Gower, *Acta Biomater.* **2011**, *7*, 3158.
[70] A. K. Burwell, T. Thula-Mata, L. B. Gower, S. Habeliz, M. Kurylo, S. P. Ho, Y. C. Chien, J. Cheng, N. F. Cheng, S. A. Gansky, S. J. Marshall, W. Grayson, *PLoS One* **2012**, *7*, e38852.
[71] T. Thula-Mata, A. Burwell, L. B. Gower, S. Habelizt, G. Marshall, *Mater. Res. Soc. Symp. Proc.* **2011**, *1355*, 1114.
[72] A. J. Lausch, B. D. Quan, J. W. Miklas, E. D. Sone, *Adv. Funct. Mater.* **2013**, *23*, 4906.
[73] H. Nurrohman, K. Saeki, K. Carneiro, Y. C. Chien, S. Djomehri, S. P. Ho, C. Qin, S. J. Marshall, L. B. Gower, G. W. Marshall, *J. Mater. Res.* **2016**, *31*, 321.
[74] H. Nurrohman, K. M. M. Carneiro, J. Hellgeth, K. Saeki, S. J. Marshall, G. W. Marshall, S. Habelitz, *PLoS One* **2017**, *12*, e0188277.
[75] A. S. Deshpande, E. Beniash, *Cryst. Growth Des.* **2008**, *8*, 3084.
[76] S. Jee, L. Culver, Y. Li, E. P. Douglas, L. B. Gower, *J. Cryst. Growth* **2010**, *312*, 1249.
[77] S. Jee, T. T. Thula, L. B. Gower, *Acta Biomater.* **2010**, *6*, 3676.
[78] S. S. Jee, R. K. Kasinath, E. DiMasi, Y.-Y. Kim, L. Gower, *CrystEngComm* **2011**, *13*, 2077.
[79] T. T. Thula, F. Svedlund, D. E. Rodriguez, J. Podschun, L. Pendi, L. B. Gower, *Polymers* **2011**, *3*, 10.
[80] Y. Li, T. T. Thula, S. Jee, S. L. Perkins, C. Aparicio, E. P. Douglas, L. B. Gower, *Biomacromolecules* **2011**, *13*, 49.
[81] Y. K. Kim, L. S. Gu, T. E. Bryan, J. R. Kim, L. Chen, Y. Liu, J. C. Yoon, L. Breschi, D. H. Pashley, F. R. Tay, *Biomaterials* **2010**, *31*, 6618.
[82] J. Chen, C. Burger, C. V. Krishnan, B. Chu, B. S. Hsiao, M. J. Glimcher, *Macromol. Chem. Phys.* **2005**, *206*, 43.
[83] K. Liang, Y. Gao, J. Lie, Y. Liao, S. Xiao, X. Zhou, J. Li, *J. Biomater. Sci., Polym. Ed.* **2015**, *26*, 963.
[84] S. Tao, M. Fan, H. H. K. Xu, J. Li, L. He, *RSC Adv.* **2017**, *7*, 54947.
[85] Y. Liu, N. Li, Y. P. Qi, L. Dai, T. E. Bryan, J. Mao, D. H. Pashley, F. R. Tay, *Adv. Mater.* **2011**, *23*, 975.
[86] F. R. Tay, D. H. Pashley, *Biomaterials* **2008**, *29*, 1127.
[87] L. S. Gu, J. Kim, Y. K. Kim, Y. Liu, S. H. Dickens, D. H. Pashley, J. Q. Ling, F. R. Tay, *Dent. Mater.* **2010**, *26*, 1077.
[88] J. Sun, C. Chen, H. Pan, Y. Chen, C. Mao, W. Wang, R. Tang, X. Gu, *J. Mater. Chem. B* **2014**, *2*, 4544.

[89] L. Gu, Y. K. Kim, Y. Liu, H. Ryou, C. E. Wimmer, L. Dai, D. D. Arola, S. W. Looney, D. H. Pashley, F. R. Tay, *J. Dent. Res.* **2011**, *90*, 82.
[90] H. Nurrohman, S. Nakashima, T. Takagaki, A. Sadr, T. Nikaido, Y. Asakawa, M. Uo, S. J. Marshall, J. Tagami, *Biomed. Mater. Eng.* **2015**, *25*, 89.
[91] L. Niu, S. E. Jee, K. Jiao, L. Tonggu, M. Li, L. Wang, Y. D. Yang, J. H. Bian, L. Breschi, S. S. Jang, J. H. Chen, D. H. Pashley, F. R. Tay, *Nat. Mater.* **2017**, *16*, 370.
[92] L. N. Niu, K. Jiao, H. Ryou, C. K. Y. Yiu, J. H. Chen, L. Breschi, D. D. Arola, D. H. Pashley, F. R. Tay, *Angew. Chem., Int. Ed.* **2013**, *52*, 5762.
[93] K. Jiao, L. Niu, Q. Li, F. Chen, W. Zhao, J. Li, J. H. Chen, C. W. Cutler, D. H. Pashley, F. R. Tay, *Acta Biomater.* **2015**, *19*, 23.
[94] L. Kalmar, D. Homola, G. Varga, P. Tompa, *Bone* **2012**, *51*, 528.
[95] A. George, A. Veis, *Chem. Rev.* **2009**, *108*, 4670.
[96] L. B. Gower, in *Biomineralization and Biomaterials: Fundamentals and Applications* (Eds: C. Aparicio, M. P. Ginebra) Woodhead Publishing, Cambridge **2015**, Ch. 6.
[97] C. Shao, R. Zhao, S. Jiang, S. Yao, Z. Wu, B. Jin, Y. Yang, H. Pan, R. Tang, *Adv. Mater.* **2018**, *30*, 1.
[98] K. Iijima, M. Hashizume, *Protein Pept. Lett.* **2018**, *25*, 25.
[99] C. Sfeir, P.-A. Fang, J. Thottala, A. Raman, Z. Xiaoyuan, E. Beniash, *Acta Biomater.* **2014**, *10*, 2241.
[100] H. Ping, H. Xie, B. Su, Y. Cheng, W. Wang, H. Wang, Y. Wang, J. Zhang, F. Zhang, Z. Fu, *J. Mater. Chem. B* **2015**, *3*, 4496.
[101] J. H. Shepherd, D. V. Shepherd, S. M. Best, *J. Mater. Sci. Med.* **2012**, *23*, 2335.
[102] M. Šupová, *Ceram. Int.* **2015**, *41*, 9203.
[103] A. Malhotra, P. Habibovic, *Trends Biotechnol.* **2016**, *34*, 983.
[104] S. Bose, G. Fielding, S. Tarafder, A. Bandyopadhyay, *Trends Biotechnol.* **2013**, *31*, 594.
[105] C. Rey, B. Collins, T. Goehl, I. R. Dickson, M. J. Glimcher, *Calcif. Tissue Int.* **1989**, *45*, 157.
[106] F. J. Martínez-Casado, M. Iafisco, J. M. Delgado-López, C. Martínez-Benito, C. Ruiz-Pérez, D. Colangelo, F. Oltolina, M. Prat, J. Gómez-Morales, *Cryst. Growth Des.* **2016**, *16*, 145.
[107] S. Lala, M. Ghosh, P. K. Das, D. Das, T. Kar, S. K. Pradhan, *Mater. Chem. Phys.* **2016**, *170*, 319.
[108] D. Laurencin, M. E. Smith, *Prog. Nucl. Magn. Reson. Spectrosc.* **2013**, *68*, 1.
[109] A. Bigi, M. Debbabi, M. Gazzano, N. Roveri, *Eur. J. Inorg. Chem.* **2001**, *5*, 1261.
[110] S. Caldarelli, J. Eon, D. Laurencin, M. E. Smith, *J. Am. Chem. Soc.* **2009**, *131*, 5145.
[111] C. Li, O. Paris, S. Siegel, P. Roschger, E. P. Paschalis, K. Klaushofer, P. Fratzl, *J. Bone Miner. Res.* **2010**, *25*, 968.
[112] A. Henss, A. Hild, M. Rohnke, S. Wenisch, J. Janek, *Biointerphases* **2016**, *11*, 02A302.
[113] M. Rohnke, A. Henss, J. Kokesch-Himmelreich, M. Schumacher, S. Ray, V. Alt, M. Gelinsky, J. Janek, *Anal. Bioanal. Chem.* **2013**, *405*, 8769.
[114] L. M. Gordon, L. Tran, D. Joester, *ACS Nano* **2012**, *6*, 10667.
[115] C. Capuccini, P. Torricelli, E. Boanini, M. Gazzano, R. Giardino, A. Bigi, *J. Biomed. Mater. Res., Part A* **2009**, *89*, 594.
[116] Z. T. Birgani, A. Malhotra, C. A. van Blitterswijk, P. Habibovic, *J. Biomed. Mater. Res., Part A* **2016**, *104*, 1946.
[117] J. Barralet, U. Gbureck, P. Habibovic, E. Vorndran, C. Gerard, C. J. Doillon, *Tissue Eng., Part A* **2009**, *15*, 1601.
[118] Y. Li, X. Chen, A. Fok, J. C. Rodriguez-Cabello, C. Aparicio, *ACS Appl. Mater. Interfaces* **2015**, *7*, 25784.
[119] Y. Li, J. C. Rodriguez-Cabello, C. Aparicio, *ACS Appl. Mater. Interfaces* **2017**, *9*, 5838.
[120] B. D. Walters, J. P. Stegemann, *Acta Biomater.* **2014**, *10*, 1488.
[121] X. Cheng, U. A. Gurkan, C. J. Dehen, M. P. Tate, H. W. Hillhouse, G. J. Simpson, O. Akkus, *Biomaterials* **2008**, *29*, 3278.
[122] J. A. Uquillas, V. Kishore, O. Akkus, *Biomed. Mater.* **2011**, *6*, 035008.
[123] J. M. Caves, V. A. Kumar, J. Wen, W. Cui, A. Martinez, R. Apkarian, J. E. Coats, K. Berland, E. L. Chaikof, *J. Biomed. Mater. Res., Part B* **2010**, *93*, 24.
[124] J. L. Ng, L. E. Knothe, R. M. Whan, U. Knothe, M. L. K. Tate, *Sci. Rep.* **2017**, *7*, 40396.
[125] J. Gilmore, T. Burg, R. E. Groff, K. J. L. Burg, *J. Biomed. Mater. Res., Part B* **2017**, *105*, 1342.
[126] S. Chen, N. Hirota, M. Okuda, M. Takeguchi, H. Kobayashi, N. Hanagata, T. Ikoma, *Acta Biomater.* **2011**, *7*, 644.
[127] J. Torbet, M. Malbouyres, N. Builles, V. Justin, M. Roulet, O. Damour, A. Oldberg, F. Ruggiero, D. J. Hulmes, *Biomaterials* **2007**, *28*, 4268.
[128] C. Guo, L. J. Kaufman, *Biomaterials* **2007**, *28*, 1105.
[129] J. Zhuang, S. Lin, L. Dong, K. Cheng, W. Weng, *ACS Biomater. Sci. Eng.* **2018**, *4*, 1528.
[130] N. Naik, J. Caves, E. L. Chaikof, M. G. Allen, *Adv. Healthcare Mater.* **2014**, *3*, 367.
[131] P. Lee, R. Lin, J. Moon, L. P. Lee, *Biomed. Microdevices* **2006**, *8*, 35.
[132] C. Haynl, E. Hofmann, K. Pawar, S. Förster, T. Scheibel, *Nano Lett.* **2016**, *16*, 5917.
[133] M. M. Giraud-Guille, G. Mosser, E. Belamie, *Curr. Opin. Colloid Interface Sci.* **2008**, *13*, 303.
[134] M. M. Giraud Guille, G. Mosser, C. Helary, D. Eglin, *Micron* **2005**, *36*, 602.
[135] Y. Wang, J. Silvent, M. Robin, F. Babonneau, A. Meddahi-Pellé, N. Nassif, M. M. Giraud Guille, *Soft Matter* **2011**, *7*, 9659.
[136] R. A. Brown, M. Wiseman, C. B. Chuo, U. Cheema, S. N. Nazhat, *Adv. Funct. Mater.* **2005**, *15*, 1762.
[137] E. A. Abou Neel, U. Cheema, J. C. Knowles, R. A. Brown, S. N. Nazhat, *Soft Matter* **2006**, *2*, 986.
[138] H. Cui, W. Zhu, M. Nowicki, X. Zhou, A. Khademhosseini, L. G. Zhang, *Adv. Healthcare Mater.* **2016**, *5*, 2174.
[139] Y. Fu, S. Liu, S. Cui, X. Kou, X. Wang, X. Liu, Y. Sun, G. Wang, Y. Liu, Y. Zhou, *ACS Appl. Mater. Interfaces* **2016**, *8*, 15958.
[140] B. Ye, X. Luo, Z. Li, C. Zhuang, L. Li, L. Lu, S. Ding, J. Tian, C. Zhou, *Mater. Sci. Eng., C* **2016**, *68*, 43.
[141] Y. Wang, N. Van Manh, H. Wang, X. Zhong, X. Zhang, C. Li, *Int. J. Nanomed.* **2016**, *11*, 2053.
[142] C. L. Duvall, W. R. Taylor, D. Weiss, A. M. Wojtowicz, R. E. Guldberg, *J. Bone Miner. Res.* **2007**, *22*, 286.
[143] A. Franzén, K. Hultenby, F. P. Reinholt, P. Önnerfjord, D. Heinegård, *J. Orthop. Res.* **2008**, *26*, 721.
[144] X. J. Luo, H. Y. Yang, L. N. Niu, J. Mao, C. Huang, D. H. Pashley, F. R. Tay, *Acta Biomater.* **2016**, *31*, 378.
[145] W. Zhang, X. J. Luo, L. N. Niu, H. Y. Yang, C. K. Y. Yiu, T. Da Wang, L. Q. Zhou, J. Mao, C. Huang, D. H. Pashley, F. R. Tay, *Sci. Rep.* **2015**, *5*, 11199.
[146] Z. Wu, X. Wang, Z. Wang, C. Shao, X. Jin, L. Zhang, H. Pan, R. Tang, B. Fu, *ACS Appl. Mater. Interfaces* **2017**, *9*, 17710.
[147] B. Cantaert, E. Beniash, F. C. Meldrum, *Chemistry* **2013**, *19*, 14918.
[148] U. G. K. Wegst, H. Bai, E. Saiz, A. P. Tomsia, R. O. Ritchie, *Nat. Mater.* **2015**, *14*, 23.
[149] M. Nakamura, S. Sone, I. Takahashi, I. Mizoguchi, S. Echigo, Y. Sasano, *J. Histochem. Cytochem.* **2005**, *53*, 1553.
[150] L. J. Foster, P. A. Zeemann, C. Li, M. Mann, O. N. Jensen, M. Kassem, *Stem Cells* **2005**, *23*, 1367.
[151] W. W. Du, L. Fang, W. Yang, W. Sheng, Y. Zhang, A. Seth, B. B. Yang, A. J. Yee, *BMC Cancer* **2012**, *12*, 341.
[152] I. Zvackova, E. Matalova, H. Lesot, *Front. Physiol.* **2017**, *8*, 554.
[153] T. Douglas, S. Heinemann, S. Bierbaum, D. Scharnweber, H. Worch, *Biomacromolecules* **2006**, *7*, 2388.
[154] Y. Mochida, D. Parisuthiman, S. Pornprasertsuk-Damrongsri, P. Atsawasuwan, M. Sricholpech, A. L. Boskey, M. Yamauchi, *Matrix Biol.* **2009**, *28*, 44.

[155] A. D. Berendsen, E. L. Pinnow, A. Maeda, A. C. Brown, N. McCartney-Francis, V. Kram, R. T. Owens, P. G. Robey, K. Holmbeck, L. F. de Castro, T. M. Kilts, M. F. Young, *Matrix Biol.* **2014**, *35*, 223.
[156] M. Myren, D. J. Kirby, M. L. Noonan, A. Maeda, R. T. Owens, S. Ricard-Blum, V. Kram, T. M. Kilts, M. F. Young, *Matrix Biol.* **2016**, *52–54*, 141.
[157] D. Parisuthiman, Y. Mochida, W. R. Duarte, M. Yamauchi, *J. Bone Miner. Res.* **2005**, *20*, 1878.
[158] T. Tashima, S. Nagatoishi, H. Sagara, S. I. Ohnuma, K. Tsumoto, *Biochem. Biophys. Res. Commun.* **2015**, *463*, 292.
[159] S. Kalamajski, A. Aspberg, K. Lindblom, D. Heinegård, Å. Oldberg, *Biochem. J.* **2009**, *423*, 53.
[160] S. Houari, T. Wurtz, D. Ferbus, D. Chateau, A. Dessombz, A. Berdal, S. Babajko, *J. Bone Miner. Res.* **2014**, *29*, 1446.
[161] S. Kalamajski, A. Oldberg, *Matrix Biol.* **2010**, *29*, 248.
[162] E. M. Rosset, A. D. Bradshaw, *Matrix Biol.* **2016**, *52–54*, 78.
[163] T. Iline-Vul, I. Matlahov, J. Grinblat, K. Keinan-Adamsky, G. Goobes, *Biomacromolecules* **2015**, *16*, 2656.
[164] K. Iba, Y. Abe, T. Chikenji, K. Kanaya, H. Chiba, K. Sasaki, T. Dohke, T. Wada, T. Yamashita, *J. Bone Miner. Metab.* **2013**, *31*, 399.
[165] A. I. Alford, A. Z. Golicz, A. L. Cathey, A. B. Reddy, *Connect. Tissue Res.* **2014**, *54*, 275.
[166] P. Gehron Robey, in *Principles of Bone Biology*, Vol. *1* (Eds: J. P. Bilezikian, L. G. Raisz, T. J. Martin), Academic Press, MA **2008**, Ch. 17.
[167] G. K. Hunter, *Calcif. Tissue Int.* **2013**, *93*, 348.
[168] G. S. Baht, G. K. Hunter, H. A. Goldberg, *Matrix Biol.* **2008**, *27*, 600.
[169] W. Bouleftour, L. Juignet, G. Bouet, R. N. Granito, A. Vanden-Bossche, N. Laroche, J. E. Aubin, M. H. Lafage-Proust, L. Vico, L. Malaval, *Matrix Biol.* **2016**, *52–54*, 60.
[170] A. A. Joshi, A. J. Chaudhari, C. Li, J. Dutta, S. R. Cherry, D. W. Shattuck, A. W. Toga, R. M. Leahy, *Nat. Genet.* **2006**, *38*, 1310.
[171] A. Nampei, J. Hashimoto, K. Hayashida, H. Tsuboi, K. Shi, I. Tsuji, H. Miyashita, T. Yamada, N. Matsukawa, M. Matsumoto, S. Morimoto, T. Ogihara, T. Ochi, H. Yoshikawa, *J. Bone Miner. Metab.* **2004**, *22*, 176.
[172] P. S. N. Rowe, *Crit. Rev. Oral Biol. Med.* **2004**, *15*, 264.
[173] M. L. Zoch, T. L. Clemens, R. C. Riddle, *Bone* **2016**, *82*, 42.
[174] J. P. Gorski, A. Wang, D. Lovitch, D. Law, K. Powell, R. J. Midura, *J. Biol. Chem.* **2004**, *279*, 25455.
[175] R. J. Midura, A. Wang, D. Lovitch, D. Law, K. Powell, J. P. Gorski, *J. Biol. Chem.* **2004**, *279*, 25464.
[176] N. T. Huffman, J. A. Keightley, C. Chaoying, R. J. Midura, D. Lovitch, P. A. Veno, S. L. Dallas, J. P. Gorski, *J. Biol. Chem.* **2007**, *282*, 26002.
[177] L. J. Schurgers, J. Uitto, C. P. Reutelingsperger, *Trends Mol. Med.* **2013**, *19*, 217.
[178] M. L. Cancela, V. Laizé, N. Conceição, *Arch. Biochem. Biophys.* **2014**, *561*, 56.
[179] Y. T. Tsao, Y. J. Huang, H. H. Wu, Y. A. Liu, Y. S. Liu, O. K. Lee, *Int. J. Mol. Sci.* **2017**, *18*, 159.
[180] A. Neve, A. Corrado, F. P. Cantatore, *J. Cell. Physiol.* **2013**, *228*, 1149.
[181] E. Mavropoulos, A. M. Costa, L. T. Costa, C. A. Achete, A. Mello, J. M. Granjeiro, A. M. Rossi, *Colloids Surf., B Biointerfaces* **2011**, *83*, 1.
[182] L. Brylka, W. Jahnen-Dechent, *Calcif. Tissue Int.* **2013**, *93*, 355.